Master Thesis

Sum Rate Analysis of Non-Orthogonal Multiple Access Systems with Residual Hardware Impairments

Afsaneh Gharouni

Institute for Digital Communications
Prof. Dr.-Ing. Robert Schober
Friedrich-Alexander-University Erlangen-Nuremberg

Supervisors: Shahram Zarei, M.Sc.
Prof. Dr.-Ing. Robert Schober

June 26, 2017

Declaration

To the best of my knowledge and belief this work was prepared without aid from any other sources except where indicated. Any reference to material previously published by any other person has been duly acknowledged. This work contains no material which has been submitted or accepted for the award of any other degree in any institution.

Erlangen, June 26, 2017

Afsaneh Gharouni
Haagstr. 17, 91054
Erlangen, Germany

Contents

Abstract

Non-Orthogonal Multiple Access (NOMA) is a promising technology which is considered as a candidate for future radio access, e.g., 5th Generation of Mobile Networks (5G). This multiplexing technique is capable of improving the system-level performance of cellular mobile communications by serving more than one user in the same time slot and frequency. In particular, supporting a heterogeneous range of Quality-of-Service (QoS) requirements, massive connectivity, and balancing the trade-off between the system throughput and user fairness are key features of NOMA which are also the requirements arising in 5G systems due to existence of applications such as Internet of Things (IoT).

The system-level performance of NOMA has been studied in literature for several scenarios. However, the effect of transceiver Hardware Impairment (HWI) has not been investigated yet. HWIs arise in real world implementations and limit the system performance. This motivates the considered topic in this thesis which is performance analysis of NOMA systems in the presence of HWIs.

In this thesis, we study the effects of transceiver HWIs on the performance of a single-cell two-user downlink NOMA system which performs Successive Interference Cancellation (SIC) at the receivers. To this end, an additive distortion model is adopted to capture the aggregate effect of residual HWIs. First, an opportunistic NOMA system is considered. There, we show that HWIs limit the system throughput of such a system, and a ceiling is derived in this regard for high-SNR regime. For the second and third scenarios, the outage probability of QoS-based and cognitive radio systems with predefined data rates is investigated. In particular, a closed-form expression is derived for the outage probability of each system for large values of SNR, and diversity gains are discussed. The system-level simulations provide numerical results to compare the performance of NOMA and conventional Orthogonal Multiple Access (OMA), and a good match between the analytical and simulation results is observed. Furthermore, simulations are performed to give an insight on NOMA gains while using more advanced power allocation and scheduling schemes.

Glossary

Abbreviations

5G	5th Generation of Mobile Networks
BS	Base Station
CR-NOMA	Cognitive Radio Non-Orthogonal Multiple Access
CSI	Channel State Information
EVM	Error Vector Magnitude
F-NOMA	Fixed Power Allocation Non-Orthogonal Multiple Access
FDMA	Frequency Division Multiple Access
FTPC	Fractional Transmission Power Allocation
HWI	Hardware Impairment
IoT	Internet of Things
MIMO	Multiple-Input Multiple-Output
NOMA	Non-Orthogonal Multiple Access
OMA	Orthogonal Multiple Access
PF	Proportional Fairness
QoS	Quality-of-Service
RF	Radio Frequency
SIC	Successive Interference Cancellation
SISO	Single-Input Single-Output
TDMA	Time Division Multiple Access
TTPA	Tree-Search Based Transmission Power Allocation

Operators

$\lvert\cdot\rvert$	Absolute value
$E\{\cdot\}$	Expected value
$\log_2$	Logarithm to base 2
$\mathcal{CN}(0,\sigma^2)$	Circular symmetric complex Gaussian distribution with zero mean and variance σ^2

Chapter 1

Introduction

The demand for higher wireless data rates has been doubled every eighteen months over the last three decades as Edholm's law suggests [1]. Thus, one requirement for future communications systems, e.g., 5G is to support even higher data rates. However, a number of new applications are also introduced to be part of these fast wireless communications such as IoT and cloud-based architectural applications. These services impose extra requirements on communications systems, such as low latency, massive connectivity and supporting heterogeneous QoS requirements [2]. Therefore, a dilemma in future communications systems is to balance the trade-off between system throughput and user fairness.

Multiple access technologies play an important role in cellular communications. That is why multiple access technologies characterize each generation of mobile communications. With OMA technologies, e.g., Time Division Multiple Access (TDMA) and Frequency Division Multiple Access (FDMA), satisfying all the mentioned requirements is so difficult, if not impossible. Therefore, breaking the orthogonality is a possible solution to allow the resources to be utilized more efficiently. In NOMA, the same time slot and subcarrier are shared by more than one user and their signals will be separated in power domain. Thus, a higher spectral efficiency and supporting larger number of users is expected. Whereas, using OMA, for example for serving a user with a poor connection to the Base Station (BS), results in low spectral efficiency.

NOMA is a promising multiple access technique which is used in 3rd Generation Partnership Project (3GPP) Long-Term Evolution Advanced (LTE-A) as Multi-User Superposition Transmission (MUST) [2] and is also included in the forthcoming digital TV standard (ATSC 3.0) [3]. Superiority of uplink NOMA vs. uplink OMA can be easily shown by information theoretical tools[1]. In addition, even for a downlink scenario with user pairing, NOMA can outperform TDMA in terms of the sum rate and individ-

[1] Refer to Appendix A for more details.

ual users' rates [4]. Therefore, NOMA has become an interesting candidate for future communications.

Authors of [5] presented the concept of NOMA and introduced it as a promising multiple access technique for future cellular radio access. Different scenarios of NOMA including single-carrier and multi-carrier schemes with different power allocations were later discussed, e.g., in [6, 7]. Uplink NOMA, cooperative NOMA and a combination of NOMA with Multiple-Input Multiple-Output (MIMO) systems have also been investigated in many papers such as [8–10]. In addition, several power allocation and scheduling methods have been proposed for NOMA systems. A number of these methods are based on iterative water-filling as in [11, 12]. In [13], an optimal joint power and subcarrier allocation for a two-user multi-carrier NOMA system was introduced.

Analyzing the performance of NOMA has also been studied for different scenarios in literature. In [14], the performance of a multi-user single-carrier NOMA system has been investigated in terms of outage probability and ergodic sum rate with perfect Channel State Information (CSI), for a cellular downlink scenario with randomly deployed users while considering a fixed power allocation. The performance of NOMA based on imperfect CSI and second order statistics is analyzed in [15]. In addition, authors of [4] have studied a two-user single-carrier system with statistical CSI from an information theoretic perspective, where it was proved that NOMA outperforms native TDMA with high probability in terms of both sum rate and individual rates.

In this thesis, we analyze the performance of downlink NOMA considering the aggregate effect of residual HWIs. HWIs are known to saturate the performance of the communications systems, e.g., massive MIMO systems [16, 17]. However, to the best of the authors' knowledge, investigation of the performance of NOMA systems with HWIs has not been considered yet. Therefore, a well-established model of HWIs is used in this thesis to study the performance degradation of NOMA systems. To this end, performance of different downlink scenarios, including opportunistic, QoS-based and Cognitive Radio Non-Orthogonal Multiple Access (CR-NOMA) are investigated in terms of sum rate and outage probability.

In particular, a NOMA system with fixed power allocation and random scheduling is adopted for the opportunistic and QoS-based scenarios. First, we consider the opportunistic NOMA where the ergodic sum rate is analyzed as the performance metric. In addition, we analyze the outage probability of a system with predefined target data rates, e.g., based on QoS requirements. Subsequently, the outage performance of CR-NOMA is analytically studied where the power allocation is performed based on the users' channel conditions. The analyses are verified by simulation results. Moreover, other NOMA

systems with Proportional Fairness (PF) scheduling and Fractional Transmission Power Allocation (FTPC) are investigated by numerical simulations, too.

The rest of this thesis is organized as follows. The downlink NOMA system with its main idea and some key features are discussed in Chapter 2. In Chapter 3, the additive distortion model is introduced and the system model which is used in this thesis is elaborated. Analytical and simulation results are presented in Chapter 4 and Chapter 5, respectively. Finally, conclusions are drawn in Chapter 6.

Chapter 2

Non-Orthogonal Multiple Access

In this chapter, basic NOMA with SIC is discussed for downlink of cellular communications systems. The main idea of downlink NOMA can be applied to an uplink scenario as well. More details on the differences between downlink and uplink NOMA can be found in [8, 18].

2.1 The Key Idea of Downlink Non-Orthogonal Multiple Access

The main concept of the downlink NOMA scenario is shown in Fig. 2.1. In NOMA, several users share the same resource block (same subband and time slot) and the signals of different users are separated in the power domain. Therefore, power allocation and scheduling play an important role in realizing NOMA gains.

In order to separate signals of different users in power domain, SIC is performed at the receivers and unlike a conventional OMA technique, more power is allocated to the weaker users. Hence, firstly the signal of the weakest user is detected at all receivers and the result is subtracted from the received signal (except for the weakest user). In order to have a tractable problem for analysis, we consider a single-carrier Single-Input Single-Output (SISO) system where the BS and all users are equipped with one antenna. The available bandwidth is 1 Hz, P is the total available power at the BS and s_j is the

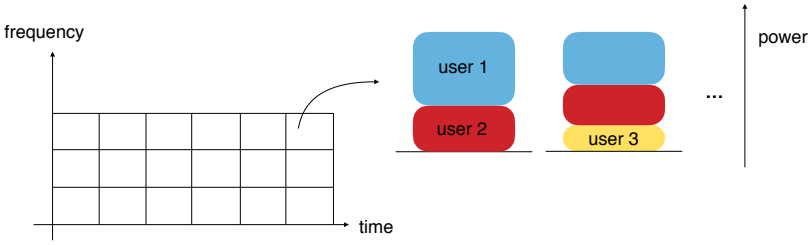

Fig. 2.1: The key idea of NOMA

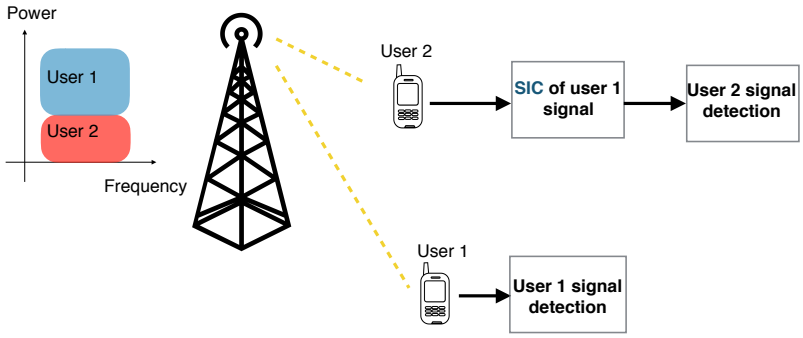

Fig. 2.2: SIC at the receivers in downlink NOMA

signal of the jth user with transmission power Pa_j, where a_j is the power coefficient of user j. The transmitted signal at the BS, which is the superposition of the users' signals, is given by

$$x_{\mathrm{BS}} = \sum_{j=1}^{M} \sqrt{a_j P} s_j, \tag{2.1}$$

where M is the number of users utilizing the available bandwidth.

Therefore, the received signal at the kth user is represented as

$$y_k = h_k x_{\mathrm{BS}} + z_k = h_k \sum_{j=1}^{M} \sqrt{a_j P} s_j + z_k, \tag{2.2}$$

where h_k is the channel gain between the kth user and the BS, $z_k \sim \mathcal{CN}(0, \sigma_{z,k}^2)$ stands for the additive white Gaussian noise at the kth user, and $s_j \sim \mathcal{CN}(0,1)$ indicates the signal of the jth user.

The optimal SIC order is in the order of the increasing channel gain normalized by the noise power [5]. In particular, if $|h_1|^2/\sigma_{z,1}^2 \leq \cdots \leq |h_M|^2/\sigma_{z,M}^2$, we have $a_1 > \cdots > a_M$ and user k can remove the inter-user interference from the $k-1$ users whose $|h_j|^2/\sigma_{z,j}^2$ is smaller than $|h_k|^2/\sigma_{z,k}^2$. Assume a simple example, where $\sigma_{z,1}^2 = \sigma_{z,2}^2$, $M = 2$ users are sharing the bandwidth and $|h_1|^2 \leq |h_2|^2$ as shown in Fig. 2.2. Since $a_1 > a_2$, the signal of user 1 can be detected first. At the stronger user, this detected signal is removed from the received signal such that the signal of the stronger user can be detected without any inter-user interference. This power allocation, which contradicts the concept of water-filling in OMA, provides fairness for the weaker user. The reason is that the signal of the stronger user, which makes more contribution in sum rate, is detected without

inter-user interference. Assuming perfect SIC and $P = 1$, the achievable rates of these two users are given by

$$R_1 = \log_2\Big(1 + \frac{a_1|h_1|^2}{\sigma_{z,1}^2 + |h_1|^2 a_2}\Big), \tag{2.3}$$

and

$$R_2 = \log_2\Big(1 + \frac{a_2|h_2|^2}{\sigma_{z,2}^2}\Big). \tag{2.4}$$

2.2 Some Advantages and Disadvantages

NOMA was proposed for 3GPP LTE-A standard [2] in order to improve the spectral efficiency in the lower frequency bands [15]. The reason is that NOMA allows users to utilize the subcarriers occupied by weak users without compromising much of their performance [2].

In addition, NOMA can simply be combined with multi-user MIMO communications systems, heterogeneous networks, small cells and networks with high mobility to improve the system performance [15], and exploits the heterogeneity of channel conditions. On top of these, NOMA can support a larger number of users with diverse QoS requirements while the weaker users, e.g., cell-edge users, benefit from better services.

Higher computational complexity and delay are some important drawbacks of NOMA due to the need for SIC process at the receivers. Furthermore, a higher inter-cell interference is expected since more power is allocated to the cell-edge users in NOMA. The requirement of CSI and power coefficients knowledge of each user for system design, and nonsignificant gains of NOMA at low SNR [14] are also some of the disadvantages.

It is worth mentioning that in order to realize the NOMA gains, e.g., high spectral efficiency and fairness, using appropriate scheduling and power allocation is vital. A number of proposed methods are discussed in the following; however, a full review goes beyond the scope of this thesis.

2.3 Power Allocation Methods

Power allocation methods for NOMA systems have a high computational complexity in general. Therefore, two heuristic suboptimal methods are discussed in this thesis: fixed power allocation and FTPC. In order to analyze the performance of NOMA in most of the simulations, fixed power allocation is adopted to keep the complexity low. In addition, we investigate the sum rate of NOMA while using FTPC to give an insight on

how much the performance can be improved if a more appropriate power allocation scheme is adopted.

2.3.1 Fixed Power Allocation

In a fixed power allocation, the transmit power of the users are selected independent of the channel conditions, e.g., $a_1 = 0.8$ and $a_2 = 0.2$ in case of $M = 2$. Another example for fixed power allocation is $a_k = \frac{M-k+1}{\mu}$ for $M > 2$ which is used in [14]. Here, μ is selected such that $\sum_{k=1}^{M} a_k = 1$. NOMA schemes using this method are denoted by Fixed Power Allocation Non-Orthogonal Multiple Access (F-NOMA) in this thesis.

2.3.2 Fractional Transmission Power Control

FTPC is similar to the power allocation method used in LTE uplink with a low computational complexity [5]. In this method, the power assigned to each user is relative to the user's channel condition as follows

$$P_k = \frac{P}{\sum_{j \in U} (|h_j|^2)^{-\alpha_{\text{FTPC}}}} \left(|h_k|^2\right)^{-\alpha_{\text{FTPC}}}, \tag{2.5}$$

where U stands for user index set, $P_k = P a_k$, and α_{FTPC} is the decay factor ($0 \leq \alpha_{\text{FTPC}} \leq 1$) which needs a priori optimization to be determined such that a target metric is maximized. It can be seen that $\alpha_{\text{FTPC}} = 0$ corresponds to equal transmit power allocation among users independent of channel conditions. On the other hand, increasing α_{FTPC} results in allocation of more power to the user with poorer channel gain. In simulations performed in this thesis, a typical value of $\alpha_{\text{FTPC}} = 0.4$ is adopted as in [5, 6].

2.4 Scheduling Methods

The scheduler selects a set of users, which share the same time/frequency resources and are separated by NOMA, where the selection is based on a specific optimization criterion. The conceptual flowchart of the combination of power allocation and scheduling for NOMA is depicted in Fig. 2.3. Clearly, an exhaustive search for scheduling imposes a very high computational complexity to the system. For example, if we assume that there are K users in the cell and M of them are allowed to access the bandwidth, $\binom{K}{1} + \binom{K}{2} + \cdots + \binom{K}{M}$ different user sets should be investigated to find the best user set based on the objective function of the scheduler. In other words, the objective function of the scheduler is computed for all sets and the set with maximum value is selected to perform NOMA on a specific subcarrier. Therefore, tolerable computational complexity is an important

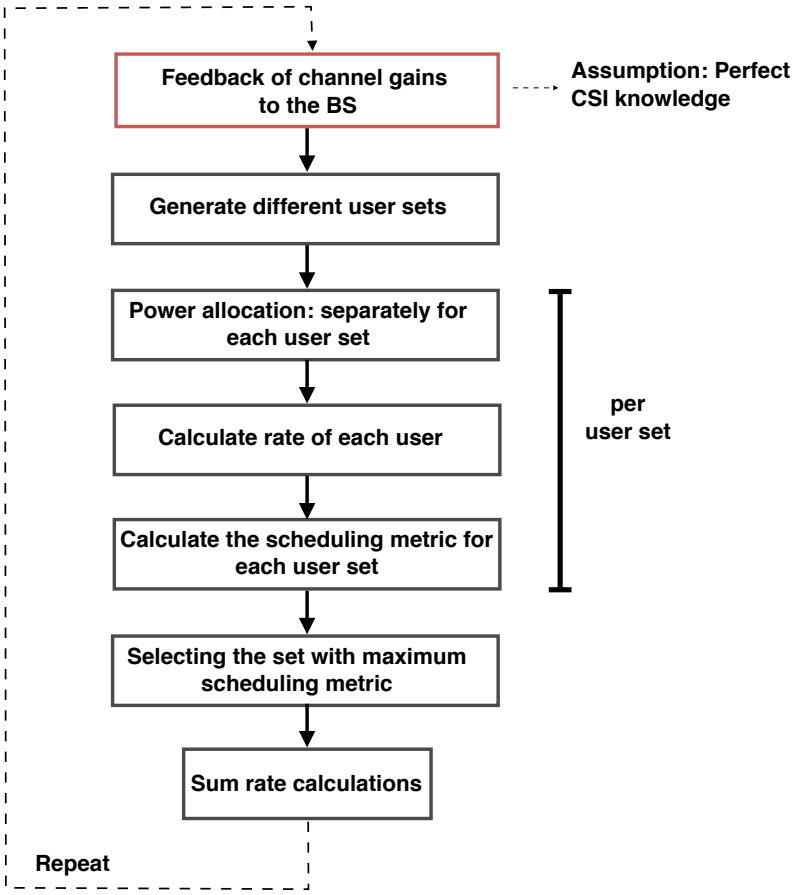

Fig. 2.3: Flowchart of the combination of power allocation and scheduling where sum rate calculations are done to investigate the system performance.

parameter to take into account when designing scheduling or power allocation techniques for NOMA systems.

In this section, we introduce some of the simple and commonly used scheduling methods in literature: pairing the most distinctive channels and PF scheduling. Note that for the sake of simplicity, a random scheduling is considered for analysis part in this thesis. These two methods are only considered briefly in the simulations.

2.4.1 Pairing the Most Distinctive Channels

Given a NOMA scenario adopting a fixed power allocation as discussed in Section 2.3.1, the scheduling/pairing method which maximizes sum rate assigns users with the most distinctive channel gains to the same set [19]. For example, if $|h_1|^2/\sigma^2_{z,1} \leq \cdots \leq |h_K|^2/\sigma^2_{z,K}$, the first and the Kth user are paired by this method.

2.4.2 Proportional Fairness Scheduling

As mentioned, a significant advantage of NOMA is to provide fairness to the weaker users in a cell and support massive connectivity. Therefore, instead of maximizing the system throughput without considering these parameters, a weighted sum rate can be maximized by a scheduler. A special case of the weighted sum rate is the objective function of the PF scheduler.

PF scheduler is known to provide a good trade-off between sum rate and user fairness [20]. This scheduling is described as follows for a single-carrier system.

$$S = \arg\max_U \underbrace{\prod_{k\in U}\Big(1+\frac{R_k}{(T-1)\bar{R}_k}\Big)}_{\text{PF metric}}, \tag{2.6}$$

where S is the selected user set and $\bar{R}_k$ indicates the average rate of user k over the time slot T. This scheduler was introduced in [20] for a multi-carrier transmission system in general.

Chapter 3

System Model

In this section, the system model is introduced. First, the HWI model is elaborated and subsequently, the general assumptions, e.g., on channel conditions are discussed. Afterwards, the system model of NOMA and OMA including their scheduling and power allocation methods are presented.

3.1 Residual Hardware Impairments

Transceiver HWIs, e.g., amplifier non-linearities, I/Q-imbalance, phase noise, and quantization errors are known to fundamentally limit the performance of communications systems [16]. In this section, we introduce a HWIs model which has been developed in [21] and captures the aggregate impact of residual HWIs, i.e., HWIs which remain after applying appropriate compensation schemes.

The residual HWI can be modelled as an additive distortion with zero-mean Gaussian distribution [16, 21]. The Gaussian distribution of HWI is clearly supported by the central limit theorem, and the accuracy of this model is verified by experimental results in [22–24]. Accordingly, the effect of HWIs on the received signal can be described as follows [21]

$$y = h(s + \eta_t) + \eta_r + z, \tag{3.1}$$

where $\eta_t \sim \mathcal{CN}(0, \sigma_t^2)$ and $\eta_r \sim \mathcal{CN}(0, \sigma_r^2)$ represent the HWIs at the transmitter and the receiver, respectively. $z \sim \mathcal{CN}(0, \sigma_z^2)$ stands for noise, s is the information symbol, and h indicates the channel.

We assume that η_t and η_r are independent of signal s, but depend on the channel h and as a result, they are stationary within each coherence period. The practicality of this model, when the impairment characteristics are static within each coherence period, can also be motivated theoretically by Bussgang theorem. This theorem shows that any nonlinear distortion function of a Gaussian signal can be reduced to an affine function where the signal is multiplied with an effective channel and corrupted by uncorrelated

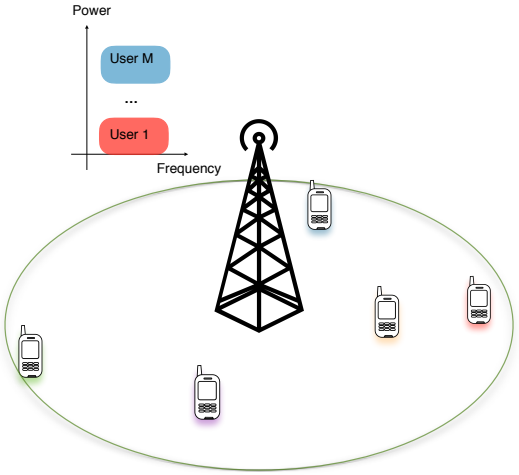

Fig. 3.1: Single-cell downlink NOMA

Gaussian noise [25]. Therefore, assuming $E\{ss^*\} = 1$, the HWI variances are given by [16]

$$\sigma_t^2 = \kappa_t E\{ss^*\} = \kappa_t, \tag{3.2}$$

$$\sigma_r^2 = \kappa_r E\{ss^*\}|h|^2 = \kappa_r |h|^2, \tag{3.3}$$

where κ_t and κ_r are the HWI parameters of the transmitter and the receiver, respectively. These parameters are determined by the quality of the Radio Frequency (RF) modules and related to the Error Vector Magnitude (EVM). EVM is a commonly used measure to characterize the severity of HWIs. For example, 3GPP LTE standard introduces a requirement on EVM to be in the range of $[0.08, 0.0175]$ [16]. Since EVM is related to the HWI parameters, e.g., $\text{EVM}_t = \sqrt{\kappa_t}$, we assume that $\kappa_t, \kappa_r \in [0.0064, 0.0306]$ in this thesis.

As can be seen from (3.2) and (3.3), the HWI variances depend on the signal power at the BS antennas and the receiver as well as the channel gain. Hence, these variances change within each coherence time of the channel implying that they are updated for different values of channel coefficients.

3.2 General Assumptions

In this thesis, we consider a single-cell downlink scenario as shown in Fig. 3.1 where the BS is located at the center of a disc with radius R serving K uniformly distributed users[1]. In addition, we assume a single-carrier transmission system with bandwidth of 1 Hz.

[1]For more details please refer to Appendix B.

Moreover, NOMA is performed for two randomly selected users ($M = 2$) in this thesis. Note that designing a multi-user NOMA system ($M > 2$) is more complicated and imposes tremendous computational complexity. On the other hand, a two-user case is capable of realizing NOMA gains and thus, considering $M = 2$ is a practical and common assumption. In addition, random scheduling is employed to make the analysis tractable. The received signal at the kth user is given by

$$y_k = h_k\Big(\sum_{j=1}^{2}\sqrt{Pa_j}s_j + \eta_t\Big) + \eta_{r,k} + z_k, \;\; k \in \{1,2\}, \tag{3.4}$$

where $z_k \sim \mathcal{CN}(0,\sigma_z^2)$ and $s_k \sim \mathcal{CN}(0,1)$ are the additive white Gaussian noise and the signal of kth user, respectively. $\eta_t \sim \mathcal{CN}(0,\kappa_t P)$ and $\eta_{r,k} \sim \mathcal{CN}(0,\kappa_{r,k}P|h_k|^2)$ denote the residual HWIs at the BS and the kth user, respectively. In additio, we assume that $h_k = g_k/\sqrt{1+d_k^{\alpha}}$ is the channel gain of the kth user where $g_k \sim \mathcal{CN}(0,1)$ represents a Rayleigh fading coefficient and the denominator denotes the path loss with d_k being the distance between the BS and the kth user and α being the path loss coefficient. We further assume that, $P = 1$ is the total transmission power of the BS and a_j is the power coefficient of the jth user while $a_1 + a_2 = 1$ always holds.

As noted before, the optimal SIC order is in the order of the increasing channel gain normalized by the noise power $|h_k|^2/\sigma_z^2$ as stated in [5] when the effect of HWI is not considered. However, taking the effect of HWIs into account influences the optimal decoding order. Since HWIs are modelled as additive distortions with Gaussian distributions, similar to noise, the optimal SIC order becomes in the order of these increasing gains $|h_k|^2/\big(\sigma_z^2+P|h_k|^2(\kappa_t+\kappa_{r,k})\big)$ or equivalently, $|h_k|^2/\big(1+\rho|h_k|^2(\kappa_t+\kappa_{r,k})\big)$ where $\rho = P/\sigma_z^2$. Without loss of generality, it is assumed that $|h_1|^2/\big(1+\rho|h_1|^2(\kappa_t+\kappa_{r,1})\big) \leq |h_2|^2/\big(1+\rho|h_2|^2(\kappa_t+\kappa_{r,2})\big)$ for the rest of this thesis.

Clearly, CSI and the knowledge of the power allocation are required in order to perform SIC. In this thesis, a perfect knowledge of both CSI and power allocation is assumed. Therefore, the achievable rates can be written as

$$R_k = \log_2\Big(1 + \frac{a_k|h_k|^2}{\sigma_z^2 + |h_k|^2(\sum_{j<k}a_j + \kappa_t + \kappa_{r,k})}\Big), \; k = 1,2, \tag{3.5}$$

conditioned on $R_{1\to 2} \geq R_1$, where $R_{1\to 2} = \log_2\Big(1+(\rho|h_2|^2a_1)/\big(1+\rho|h_2|^2(a_2+\kappa_t+\kappa_{r,2})\big)\Big)$ denotes the rate for user 1 which can be detected at user 2. As shown in the following, this condition always holds if the SIC order is obtained based on $|h_k|^2/\big(1+\rho|h_k|^2(\kappa_t+\kappa_{r,k})\big)$.

$$
\begin{aligned}
&|h_1|^2/\big(\sigma_z^2+|h_1|^2P(\kappa_t+\kappa_{r,1})\big) \le |h_2|^2/\big(\sigma_z^2+|h_2|^2P(\kappa_t+\kappa_{r,2})\big) \\
&\iff |h_1|^2\sigma_z^2+|h_1h_2|^2P(\kappa_t+\kappa_{r,2}) \le |h_2|^2\sigma_z^2+|h_1h_2|^2P(\kappa_t+\kappa_{r,1}) \qquad (3.6)\\
&\iff |h_1|^2\sigma_z^2+|h_1h_2|^2P(a_2+\kappa_t+\kappa_{r,2}) \le |h_2|^2\sigma_z^2+|h_1h_2|^2P(a_2+\kappa_t+\kappa_{r,1}) \\
&\iff \frac{1}{|h_1|^2\sigma_z^2+|h_1h_2|^2P(a_2+\kappa_t+\kappa_{r,2})} \ge \frac{1}{|h_2|^2\sigma_z^2+|h_1h_2|^2P(a_2+\kappa_t+\kappa_{r,1})} \\
&\iff \frac{1}{|h_1|^2(\sigma_z^2+|h_2|^2P(a_2+\kappa_t+\kappa_{r,2}))} \ge \frac{1}{|h_2|^2(\sigma_z^2+|h_1|^2P(a_2+\kappa_t+\kappa_{r,1}))} \\
&\iff \frac{Pa_1|h_2|^2}{\sigma_z^2+|h_2|^2P(a_2+\kappa_t+\kappa_{r,2})} \ge \frac{Pa_1|h_1|^2}{\sigma_z^2+|h_1|^2P(a_2+\kappa_t+\kappa_{r,1})} \\
&\iff R_{1\to2} \ge R_1. \qquad (3.7)
\end{aligned}
$$

3.3 Non-Orthogonal Multiple Access

In this thesis, we consider two types of F-NOMA. First, we investigate ergodic sum rate of an opportunistic NOMA scenario. In the next part, the outage probability is investigated as the performance metric for predefined target data rates in a QoS-based system. The fixed power allocation adopted for both of these types is $a_1 = 0.8$ and a_2=0.2. These two types are elaborated in the following.

Type 1: Users' data rates R_k are determined opportunistically according to their channel conditions. Therefore, no outage occurs and system performance is described in terms of ergodic sum rate as follows

$$
R_{\text{avg}} = \int_0^\infty \sum_{k=1}^{2} \log_2\Big(1+\frac{\rho a_k y}{1+\rho y(\sum_{j<k} a_j+\kappa_t+\kappa_{r,k})}\Big) f_y(Y)\mathrm{d}y, \qquad (3.8)
$$

where $f_y(Y)$ stands for the Probability Density Function (PDF) of $|h_k|^2$ for $k = 1, 2$.

Type 2: Target data rates $\tilde{R}_k$ are determined for users based on their QoS requirements. In this case, it is important to investigate the probability of the following events: Probability that the target data rate of each user is not larger than its achievable rate ($R_k \ge \tilde{R}_k$), i.e. user's QoS requirements can be satisfied. And, the other event is to ensure that the signal of the weaker user can be detected at the stronger user ($R_{1\to2} \ge \tilde{R}_1$).

Note that it is important to calculate the outage probability in this case, and that the sum rate is not of interest because it is simply sum of the target data rates. A full description of outage probability is presented in Chapter 4.

In addition to the two F-NOMA scenarios, we consider a CR-NOMA system in this thesis. In this case, NOMA is performed for a strong user and a primary user which has a

predefined target data rate and poor channel condition. Therefore, the power allocation of this scenario is performed dynamically based on the target data rate and the channel condition of the primary user. The power coefficients and the outage probability of this system are derived in Section 4.3.

3.4 Orthogonal Multiple Access

The OMA techniques which are considered in literature in order to provide a fair comparison, use the same scheduling and power allocation as the one used for NOMA [5–8, 11, 13, 14], e.g., proportional fairness scheduler and FTPC/Tree-Search Based Transmission Power Allocation (TTPA) is assumed for both multiple access techniques. However, these papers typically propose a power allocation and/or scheduling method and provide numerical results.

In this thesis, we consider a randomly scheduled OMA, similar to the considered NOMA scenario, while the available resources are divided equally between the users. Without considering the effects of HWIs, the achievable rates for OMA users are given by

$$R_k = \frac{1}{2}\log_2(1+\rho|h_k|^2). \tag{3.9}$$

And if HWIs are present, the achievable rates can be written as follows

$$R_k = \frac{1}{2}\log_2\Big(1+\frac{\rho|h_k|^2}{1+\rho|h_k|^2(\kappa_t+\kappa_{r,k})}\Big),\ \ k\in\{1,2\}. \tag{3.10}$$

Chapter 4

Performance Analysis

4.1 Asymptotic Sum Rate Analysis for Fixed Power Allocation

The system model and assumptions for type 1 of the F-NOMA is elaborated in Section 3.3. As previously mentioned, the ergodic sum rate of such system can be written as follows

$$R_{\text{avg}} = \int_0^{\infty} \sum_{k=1}^{2} \log_2\Big(1 + \frac{\rho a_k y}{1 + \rho y(\sum_{j<k} a_j + \kappa_t + \kappa_{r,k})}\Big) f_y(Y)\mathrm{d}y. \tag{4.1}$$

It is known that the effects of HWIs, limit the system performance [16]. In addition, investigating the performance in high-SNR regime provides insight and it is more tractable as well. Therefore, the focus of our analysis is on high-SNR scenarios in this thesis. In particular, when $\rho \to \infty$ and using L' Hopital's rule, we can write

$$\begin{aligned}\tilde{R}_{\text{avg,NOMA}} &= \lim_{\rho\to\infty} \sum_{k=1}^{2} \int_0^{\infty} \log_2\Big(1 + \frac{\rho a_k y}{1 + \rho y(\sum_{j<k} a_j + \kappa_t + \kappa_{r,k})}\Big) f_y(Y)\mathrm{d}y \\ &= \underbrace{\sum_{k=1}^{2} \log_2\Big(1 + \frac{a_k}{\sum_{j<k} a_j + \kappa_t + \kappa_{r,k}}\Big)}_{\downarrow \text{ ceiling}}.\end{aligned} \tag{4.2}$$

It can be seen that the performance of NOMA is saturated by the ceiling of (4.2) when the effect of HWIs is considered. Higher values of κ_t and $\kappa_{r,k}$ result in a lower ceiling on the sum rate at high-SNR values. Note that the constant ceiling derived in (4.2) is only valid for a fixed power allocation, i.e., when a_k does not depend on channel conditions.

Considering the achievable rate of OMA as given by (3.9) and by taking the integral over all possible channel realizations similar to (4.1), the ergodic sum rate of OMA at high-SNR regime can be described as follows

$$\tilde{R}_{\text{avg,OMA}} = \frac{1}{2}\sum_{k=1}^{2}\log_2\Big(1+\frac{1}{\kappa_t+\kappa_{r,k}}\Big). \tag{4.3}$$

4.2 Outage Probability Analysis for Fixed Power Allocation

Type 2 of F-NOMA was described in Section 3.3. In this section, two users with $\kappa_{r,(1)}$ and $\kappa_{r,(2)}$ are considered. After computing users' gains for determining the SIC order, HWI parameter of the receiver of the weaker user is shown by $\kappa_{r,1}$ which can be equal to either $\kappa_{r,(1)}$ or $\kappa_{r,(2)}$. In addition, target data rates of $\tilde{R}_1$ and $\tilde{R}_2$ are determined for the weaker and the stronger user, respectively.

Assuming that the jth user comes before the mth user in the decoding order, the system performance can be investigated by studying the probability that a user can cancel other users' messages ($R_{j\to m} \geq \tilde{R}_j$ for $m \in \{1,2\}$ and $j < m$) and the QoS requirement is satisfied for each user $R_j \geq \tilde{R}_j$. Therefore, we define the outage event as $E_{m,j} = \{R_{j\to m} < \tilde{R}_j\}$ and its complementary set as $E^c_{m,j}$. The outage probability at the mth user can be expressed as

$$\mathrm{P}_m^{\text{out}} = 1 - \mathrm{P}\{\cap_{j=1}^{m} E^c_{m,j}\}. \tag{4.4}$$

By defining $x_j \triangleq \frac{|h_j|^2}{1+\rho|h_j|^2(\kappa_t+\kappa_{r,j})}$ for $j=1,2$, the complementary set of outage event is given by

$$\begin{aligned}
E^c_{m,j} &= \Big\{\frac{\rho|h_m|^2 a_j}{1+\rho|h_m|^2(\sum_{i>j}a_i+\kappa_t+\kappa_{r,m})} \geq \phi_j\Big\} \\
&= \Big\{\rho|h_m|^2 a_j \geq \phi_j + \phi_j\rho|h_m|^2\sum_{i>j}a_i + \phi_j\rho|h_m|^2(\kappa_t+\kappa_{r,m})\Big\} \\
&= \{\frac{\rho|h_m|^2 a_j}{1+\rho|h_m|^2(\kappa_t+\kappa_{r,m})} \geq \phi_j\frac{1+\rho|h_m|^2\sum_{i>j}a_i+\rho|h_m|^2(\kappa_t+\kappa_{r,m})}{1+\rho|h_m|^2(\kappa_t+\kappa_{r,m})}\} \\
&= \{\rho a_j x_m \geq \phi_j(1+\rho x_m\sum_{i>j}a_i)\} \\
&\underset{(a)}{=} \{x_m \geq \frac{\phi_j}{\rho(a_j-\phi_j\sum_{i>j}a_i)}\},
\end{aligned} \tag{4.5}$$

where $\phi_j = 2^{\tilde{R}_j} - 1$. Note that step (a) is achieved assuming that $a_j > \phi_j \sum_{i>j} a_i$ holds. This condition reduces to $a_1 > \phi_1 a_2$ for $M = 2$, and it is equivalent to $\tilde{R}_1 \leq 2.32$ bit per channel use for the fixed power allocation that we adopt here.

By defining $\psi_j \triangleq \frac{\phi_j}{\rho(a_j - \phi_j \sum_{i>j} a_i)}$ and $\psi_m^* \triangleq \max\{\psi_1, \cdots \psi_m\}$ the outage probability can be stated as follows

$$\mathrm{P}_m^{\mathrm{out}} = 1 - \mathrm{P}\{x_m \geq \psi_m^*\} = F_{x_m}(\psi_m^*), \tag{4.6}$$

where $F_{x_m}(X)$ stands for the Cumulative Distribution Function (CDF) of the mth gain (x_m). Here, the outage probability of the stronger user (user 2) and the weaker user (user 1) are calculated separately. For the first user, i.e., for $m = 1$, and considering that $x_{(1)}$ and $x_{(2)}$ are independent random variables since $|h_1|^2$ and $|h_2|^2$ are independent, we have

$$\begin{aligned}
\mathrm{P}_1^{\mathrm{out}} &= 1 - \mathrm{P}\{x_1 \geq \psi_1^*\} \\
&= 1 - \mathrm{P}\{x_{(1)} \geq \psi_1^*, x_{(2)} \geq \psi_1^*\} \\
&= 1 - \mathrm{P}\{x_{(1)} \geq \psi_1^*\}\mathrm{P}\{x_{(2)} \geq \psi_1^*\} \\
&= 1 - \big(1 - F_{x_{(1)}}(\psi_1^*)\big)\big(1 - F_{x_{(2)}}(\psi_1^*)\big).
\end{aligned} \tag{4.7}$$

As can be seen, the CDFs of the unordered gains $F_{x_{(k)}}(X)$ are needed to calculate P_1^{out}. These CDFs can be derived from $F_y(Y) \triangleq F_{|h|^2}(Y)$, which is given in [14] as

$$F_y(Y) = \frac{2}{R^2} \int_0^R (1 - e^{-Y(1+y^\alpha)}) y \mathrm{d}y. \tag{4.8}$$

The elementary function of this integral is approximated in [14] using Gaussian-Chebyshev quadrature. However, here we investigate the approximation $e^x = \sum_{i=0}^{\infty} \frac{x^i}{i!}$ which provides us with a better precision of the outage probability at high-SNRs according to the simulations. The final solutions using both methods are described in Section 4.2.1 and 4.2.2, respectively. In addition, another solution is provided in Section 4.2.3 using incomplete gamma function.

4.2.1 Power Series Based Solution

In this section, in order to solve the integral of (4.8), the approximation $e^{-Yy^{\alpha}} = \sum_{i=0}^{\infty} \frac{(-Yy^{\alpha})^i}{i!}$ is utilized. Thus, (4.8) can be rewritten as

$$\begin{aligned} F_y(Y) &= \frac{2}{R^2}\int_0^R y\mathrm{d}y - \frac{2e^{-Y}}{R^2}\int_0^R e^{-Yy^{\alpha}} y\mathrm{d}y \qquad (4.9)\\ &= 1 - \frac{2e^{-Y}}{R^2}\int_0^R \sum_{i=0}^{\infty}\frac{(-Yy^{\alpha})^i}{i!} y\mathrm{d}y \\ &= 1 - \frac{2e^{-Y}}{R^2}\sum_{i=0}^{\infty}\int_0^R \frac{(-Y)^i y^{i\alpha+1}}{i!}\mathrm{d}y \\ &= 1 - \frac{2e^{-Y}}{R^2}\sum_{i=0}^{\infty}\frac{(-Y)^i}{i!}\Big[\frac{y^{i\alpha+2}}{i\alpha+2}\Big]_0^R \\ &= 1 - \frac{2e^{-Y}}{R^2}\sum_{i=0}^{\infty}\frac{(-Y)^i}{i!}\frac{R^{i\alpha+2}}{i\alpha+2}. \qquad (4.10) \end{aligned}$$

In addition, we have

$$\begin{aligned} x_{(k)} &= \frac{|h|^2}{1+\rho(\kappa_t+\kappa_{r,(k)})|h|^2} \\ &= \frac{y}{1+c_{(k)}y}, \qquad (4.11) \end{aligned}$$

where $c_{(k)} \triangleq \rho(\kappa_t+\kappa_{r,(k)})$ and $y = |h|^2$ stands for unordered channel gains. Since $x_{(k)}$ is an increasing function of y, and y is a continuous variable in $[0,\infty)$, $F_{x_{(k)}}(X)$ can be written as[1]

$$F_{x_{(k)}}(X) = \mathrm{P}\{u(y)\le X\} = \mathrm{P}\{y\le u^{-1}(X)\} = F_y\Big(\frac{X}{1-c_{(k)}X}\Big). \qquad (4.12)$$

Using (4.10) and (4.12), P_1^{out} is given by

$$P_1^{\text{out}} = 1 - \Big(\frac{2e^{-\frac{\psi_1^*}{1-c_{(1)}\psi_1^*}}}{R^2}\sum_{i=0}^{\infty}\frac{(-\frac{\psi_1^*}{1-c_{(1)}\psi_1^*})^i}{i!}\frac{R^{i\alpha+2}}{i\alpha+2}\Big)\Big(\frac{2e^{-\frac{\psi_1^*}{1-c_{(2)}\psi_1^*}}}{R^2}\sum_{i=0}^{\infty}\frac{(-\frac{\psi_1^*}{1-c_{(2)}\psi_1^*})^i}{i!}\frac{R^{i\alpha+2}}{i\alpha+2}\Big). \qquad (4.13)$$

[1] Since we know $0\le y<\infty$, it can be concluded that $0\le x_{(k)}\le\frac{1}{c_{(k)}}$ where $1/c_{(k)} = 1/\big(\rho(\kappa_t+\kappa_{r,(k)})\big)$.

Furthermore, P_2^{out} can be written as follows

$$\begin{aligned}
P_2^{\text{out}} =& \mathrm{P}\{x_2 \le \psi_2^*\} \\
=& \mathrm{P}\{x_{(1)} \le \psi_2^*, x_{(2)} \le \psi_2^*\} \\
=& F_{x_{(1)}}(\psi_2^*) \times F_{x_{(2)}}(\psi_2^*) \\
=& \Big(1 - \frac{2e^{-\frac{\psi_2^*}{1-c_{(1)}\psi_2^*}}}{R^2} \sum_{i=0}^{\infty} \frac{(-\frac{\psi_2^*}{1-c_{(1)}\psi_2^*})^i}{i!} \frac{R^{i\alpha+2}}{i\alpha+2}\Big) \\
& \times \Big(1 - \frac{2e^{-\frac{\psi_2^*}{1-c_{(2)}\psi_2^*}}}{R^2} \sum_{i=0}^{\infty} \frac{(-\frac{\psi_2^*}{1-c_{(2)}\psi_2^*})^i}{i!} \frac{R^{i\alpha+2}}{i\alpha+2}\Big).
\end{aligned} \tag{4.14}$$

Since the results of (4.13) and (4.14) are too complicated to gain insights, we investigate the asymptotic behaviour of P_1^{out} and P_2^{out}. For high values of SNR, i.e., for $\rho \to \infty$, we have $c_{(k)} = \rho(\kappa_t + \kappa_{r,(k)}) \to \infty$ and therefore, $x \to 0$ and $Y = \frac{X}{1-c_{(k)}X} \to 0$. Hence, the exponential terms in $F_y(Y)$ can be approximated by changing $\sum_0^\infty$ to $\sum_0^N$. Here, we assume $N = 1$ and thus, we have $e^{-Y} \approx 1 - Y$ and $e^{-Yy^\alpha} \approx 1 - Yy^\alpha$. By substituting these terms in (4.9), $F_y(Y)$ can be expressed as follows

$$\begin{aligned}
F_y(Y) &= 1 - \frac{2(1-Y)}{R^2} \int_0^R (1 - Yy^\alpha) y \mathrm{d}y \\
&= 1 - \frac{2(1-Y)}{R^2}\Big[\frac{R^2}{2} - Y\frac{R^{\alpha+2}}{\alpha+2}\Big] \\
&= 1 - \frac{2(1-Y)}{R^2}\Big[\frac{R^2(\alpha+2-2YR^\alpha)}{2(\alpha+2)}\Big] \\
&= 1 - \frac{(1-Y)(\alpha+2-2YR^\alpha)}{\alpha+2} \\
&= \frac{1}{\alpha+2}\Big[-2R^\alpha Y^2 + (2R^\alpha + \alpha + 2)Y\Big].
\end{aligned} \tag{4.15}$$

Using (4.15), estimations of $F_{x_{(k)}}$ can be easily derived from (4.12) and outage probabilities can be approximated as

$$\begin{aligned}
P_1^{\text{out}} =& 1 - \big(1 - F_{x_{(1)}}(\psi_1^*)\big)\big(1 - F_{x_{(2)}}(\psi_1^*)\big) \\
\approx& 1 - \Big(\frac{2R^\alpha(\frac{\psi_1^*}{1-c_{(1)}\psi_1^*})^2 + (2R^\alpha - \alpha - 2)(\frac{\psi_1^*}{1-c_{(1)}\psi_1^*}) - \alpha - 2}{-(\alpha+2)}\Big) \\
& \times \Big(\frac{2R^\alpha(\frac{\psi_1^*}{1-c_{(2)}\psi_1^*})^2 + (2R^\alpha - \alpha - 2)(\frac{\psi_1^*}{1-c_{(2)}\psi_1^*}) - \alpha - 2}{-(\alpha+2)}\Big),
\end{aligned} \tag{4.16}$$

$$
\begin{aligned}
P_2^{\text{out}} =& F_{x_{(1)}}(\psi_2^*) \times F_{x_{(2)}}(\psi_2^*)\big) \\
\approx& \frac{1}{(\alpha+2)^2}\Big[-2R^\alpha\big(\frac{\psi_2^*}{1-c_{(1)}\psi_2^*}\big)^2+(2R^\alpha+\alpha+2)\big(\frac{\psi_2^*}{1-c_{(1)}\psi_2^*}\big)\Big] \\
&\times\Big[-2R^\alpha\big(\frac{\psi_2^*}{1-c_{(2)}\psi_2^*}\big)^2+(2R^\alpha+\alpha+2)\big(\frac{\psi_2^*}{1-c_{(2)}\psi_2^*}\big)\Big]. \qquad (4.17)
\end{aligned}
$$

Diversity gains of this scheme without HWIs are 1 and 2 for the weaker and the stronger user as analyzed in [14]. Thus, diversity gain of NOMA is generally larger than the diversity gain of the introduced OMA which is equal to one. Here, it can be seen that when $\rho \to \infty$, limits of the two outage probabilities can be written as $\lim_{\rho\to\infty} P_1^{\text{out}} = \sum_{i=1}^{4} \eta_i \rho^{-i}$ and $\lim_{\rho\to\infty} P_2^{\text{out}} = \sum_{i=2}^{4} \eta_i \rho^{-i}$ while $\eta_i \neq 0$. Therefore, the terms which limit the speed of outage probabilities to approach 0 when $\rho \to \infty$, are $\frac{1}{\rho}$ and $\frac{1}{\rho^2}$ for the weak and the strong users, respectively. This implies that the diversity gains of 1 and 2 are achieved and NOMA is showing reliability to HWI effects in this sense. Clearly, in NOMA systems, each user has a different diversity gain which depends on the user's decoding order. Note that this method is referred to as method 1 in simulations.

4.2.2 Gaussian-Chebyshev Quadrature Based Solution

As mentioned, the integral of (4.8) can also be estimated using Gaussian-Chebyshev quadrature [14] as follows

$$
\begin{aligned}
F_y(Y) &= \frac{2}{R^2}\int_0^R (1-e^{-Y(1+y^\alpha)})y\,\mathrm{d}y \\
&\approx \frac{1}{R}\sum_{n=1}^{N} w_n g(\theta_n), \qquad (4.18)
\end{aligned}
$$

where $w_n = \frac{\pi}{N}$, $g(x) = \sqrt{1-x^2}(1-e^{-c_n Y})(\frac{R}{2}x+\frac{R}{2})$, $\theta_n = \cos(\frac{2n-1}{2N}\pi)$ and $c_n = 1+(\frac{R}{2}\theta_n+\frac{R}{2})^\alpha$. For large values of SNR, and by applying $e^{-Y(1+y^\alpha)} \approx 1+Y(1+y^\alpha)$, (4.18) can be approximated as

$$
F_y(Y) \approx \frac{1}{R}\sum_{n=1}^{N} \beta_n Y, \qquad (4.19)
$$

where $\beta_n = w_n\sqrt{1-\theta_n^2}(\frac{R}{2}\theta_n + \frac{R}{2})c_n$. Therefore, outage probabilities are given by

$$P_1^{\text{out}} \approx 1-(1-\frac{1}{R}\sum_{n=1}^{N}\beta_n\frac{\psi_1^*}{1-c_{(1)}\psi_1^*})(1-\frac{1}{R}\sum_{n=1}^{N}\beta_n\frac{\psi_1^*}{1-c_{(2)}\psi_1^*})$$
$$=(\frac{1}{R}\sum_{n=1}^{N}\beta_n)^2(\frac{\psi_1^*}{1-c_{(1)}\psi_1^*}\times\frac{\psi_1^*}{1-c_{(2)}\psi_1^*})+\frac{1}{R}\sum_{n=1}^{N}\beta_n(\frac{\psi_1^*}{1-c_{(1)}\psi_1^*}+\frac{\psi_1^*}{1-c_{(2)}\psi_1^*}). \quad (4.20)$$

$$P_2^{\text{out}} \approx (\frac{1}{R}\sum_{n=1}^{N}\beta_n\frac{\psi_2^*}{1-c_{(1)}\psi_2^*})(\frac{1}{R}\sum_{n=1}^{N}\beta_n\frac{\psi_2^*}{1-c_{(2)}\psi_2^*}). \quad (4.21)$$

From (4.20) and (4.21), it can be seen that the terms which limit the speed of outage probabilities, which approach 0 when $\rho \to \infty$, are $\frac{1}{\rho}$ and $\frac{1}{\rho^2}$ for the weak and the strong user, respectively. In other words, diversity gains are 1 for the weak user and 2 for the strong user. These results match with those derived from the first method. This Gaussian-Chebyshev quadrature based solution is referred to as method 2 in simulations.

4.2.3 Gamma Function Based Solution

We can also calculate the integral of (4.8) using incomplete gamma function as in $\int x^m e^{-\beta x^n} = -\frac{\Gamma(\lambda,\beta x^n)}{n\beta^\lambda}$, where $n \neq 0$ and $\beta \neq 0$. Since for the case under study $\alpha \neq 0$ and $Y = |h^2| \neq 0$, we can write

$$F_y(Y) = \frac{2}{R^2}\int_0^R y\,\mathrm{d}y - \frac{2e^{-Y}}{R^2}\int_0^R e^{-Yy^\alpha}y\,\mathrm{d}y$$
$$= 1+\frac{2e^{-Y}}{R^2}\frac{\Gamma(\lambda, Yy^\alpha)}{\alpha Y^\lambda}, \quad (4.22)$$

where $\lambda = \frac{1+1}{\alpha}$ and $\Gamma(\cdot,\cdot)$ stands for incomplete gamma function. The result of this method does not provide appropriate insight and thus, is not presented here.

4.3 Outage Probability Analysis for Cognitive Radio NOMA

In this section, the outage probability performance of a CR-NOMA system suffering from HWIs is investigated. In CR-NOMA which was analyzed in [26] for ideal hardware, a primary user which has a high priority and a poor channel condition is served by the BS based on a QoS requirement or equivalently, a specific target data rate $\tilde{R}_1$. Several

conditions may be considered as a reason for the high priority of the weak users, e.g., improving the fairness. In this case, a strong user can be served in the same frequency band as that of the primary user to enhance the spectral efficiency. This stronger user is called cognitive radio user in this context.

In order to perform analysis, same parameters and system model are assumed as in Section 3.1 and 3.2. In addition, we define $\kappa_1 = \kappa_t + \kappa_{r,1}$ and $\kappa_2 = \kappa_t + \kappa_{r,2}$ which belong to the primary and the cognitive radio user, respectively. Here, the condition on the target data rate of the primary user must hold and therefore,

$$\tilde{a}_1 = \frac{\rho y_1 \phi_1 (1+\kappa_1) + \phi_1}{\rho y_1 (1+\phi_1)}, \tag{4.23}$$

where $y_1 = |h_1|^2$ and $\phi_1 = 2^{\tilde{R}_1} - 1$. In case $\tilde{a}_1 > P$, the total power of the BS is allocated to the primary user. Therefore, $a_1 = \min\{\tilde{a}_1, 1\}$ since $P = 1$ is assumed. The rest of the power of the BS can be used by the stronger user according to $a_2 = \max\{0, \tilde{a}_2\}$ where $\tilde{a}_2 = 1 - \tilde{a}_1$. Hence, we have

$$\tilde{a}_2 = \frac{\rho y_1 (1-\kappa_1 \phi_1) - \phi_1}{\rho y_1 (1+\phi_1)}. \tag{4.24}$$

Clearly, the outage probability of the stronger user is of interest since the QoS of the primary user is met due to the choice of a_1. The outage probability of the cognitive radio user is defined as

$$P_2^{\text{out}} = \underbrace{\mathrm{P}\{\tilde{a}_2 \leq 0\}}_{Q_1} + \underbrace{\mathrm{P}\{\tilde{a}_2 > 0, \frac{\rho \tilde{a}_2 y_2}{1+\rho y_2 \kappa_2} < \phi_2\}}_{Q2}, \tag{4.25}$$

where $y_2 = |h_2|^2$ and $\phi_2 = 2^{\tilde{R}_2} - 1$. In this cognitive radio scenario, it is assumed that the target data rate of the primary user satisfies $1 - \kappa_1 \phi_1 > 0$ for all values of $\kappa_1 \in [\kappa_{\min}, \kappa_{\max}]$ because otherwise, the outage probability of user 2 always approaches 1 since $\tilde{a}_2 < 0$ will always holds based on (4.24).

The event of $\tilde{a}_2 \leq 0$ in Q_1 holds if

$$y_1 \leq \frac{\phi_1}{\rho(1-\kappa_1 \phi_1)} \triangleq \epsilon_1. \tag{4.26}$$

In addition, the event of $R_2 < \tilde{R}_2$ in Q_2 can be written as

$$\begin{aligned}
&\rho y_2\left(\frac{\rho y_1(1-\kappa_1\phi_1)-\phi_1}{\rho y_1(1+\phi_1)}\right) < \phi_2 + \rho y_2\kappa_2\phi_2,\\
\Rightarrow &\rho y_2\left(\frac{1-\kappa_1\phi_1}{1+\phi_1} - \kappa_2\phi_2 - \frac{\phi_1}{\rho(1+\phi_1)y_1}\right) < \phi_2,\\
\Rightarrow &\rho y_2\left(b - \frac{a}{y_1}\right) < \phi_2,\\
\Rightarrow &b\rho y_2 y_1 - a\rho y_2 < \phi_2 y_1,\\
\Rightarrow &\rho y_1\left(b y_2 - \frac{\phi_2}{\rho}\right) < a\rho y_2,\\
\overset{(a)}{\Rightarrow} &b y_1 < a,
\end{aligned} \tag{4.27}$$

where $a \triangleq \frac{\phi_1}{\rho(1+\phi_1)}$. Note that step (a) in (4.27) is written assuming $\rho \to \infty$ and consequently, $\phi_2/\rho \to 0$. Obviously, (4.27) always holds for $b \leq 0$. However, it is equivalent to $y_1 < a/b$ for $b > 0$.

Moreover, the optimum SIC order must hold for two users participating in CR-NOMA as follows

$$\frac{y_1}{1+\rho y_1\kappa_1} < \frac{y_2}{1+\rho y_2\kappa_2}. \tag{4.28}$$

This decoding order which will be referred to as $x_1 < x_2$ imposes more constraints on (4.25).

Here, we consider four cases based on the system parameters κ_k, ϕ_k, $k \in \{1,2\}$. By defining $\Delta\kappa \triangleq \kappa_2 - \kappa_1$ and $b \triangleq \frac{1-\kappa_1\phi_1}{1+\phi_1} - \kappa_2\phi_2$, these cases are given as follows.

1. $\Delta\kappa > 0$ **and** $b > 0$
2. $\Delta\kappa > 0$ **and** $b < 0$
3. $\Delta\kappa < 0$ **and** $b < 0$
4. $\Delta\kappa < 0$ **and** $b > 0$

For satisfying $x_1 < x_2$ as in (4.28) at high SNR, $\kappa_2 < \kappa_1$ or equivalently, $\Delta\kappa < 0$ should hold. According to simulations, the occurrence of $x_1 < x_2$ is rare for $\Delta\kappa > 0$, i.e., the probability is smaller than 2% for 10^6 channel realizations. As a result, case 1 and 2 are not of interest for practical scenarios. This implies that in order to achieve NOMA gains, a user with better HWI parameter should be selected for pairing with the primary user in high-SNR regime since in this case, the optimal SIC order condition is met for most of the channel realizations. Hence, we analyze the performance of case 3 and 4 in the following.

Case 3: $\Delta\kappa < 0$ **and** $b < 0$**:**

For $\Delta\kappa < 0$, (4.28) can be reformulated as $y_2 > \frac{y_1}{1-\rho y_1 \Delta\kappa} \rightarrow 1/(\rho\Delta\kappa)$ in high-SNR regime. In this case, Q_1 and Q_2 can be stated as

$$Q_1 = \mathrm{P}\{y_1 \leq \epsilon_1, y_2 > 1/(\rho\Delta\kappa)\}, \tag{4.29}$$

and considering (4.27)

$$Q_2 = \mathrm{P}\{y_1 > \epsilon_1, y_2 > 1/(\rho\Delta\kappa)\}. \tag{4.30}$$

Since y_1 and y_2 are independent variables, Q_1 and Q_2 can be written as product of probabilities and therefore, the outage probability of the cognitive radio user can be written as follows

$$\begin{aligned} P_2^{\text{out}} =& \mathrm{P}\{y_2 > 1/(\rho\Delta\kappa)\} \times \Big(\mathrm{P}\{y_1 \leq \epsilon_1\} + \mathrm{P}\{y_1 > \epsilon_1\}\Big) \\ =& \mathrm{P}\{y_2 > 1/(\rho\Delta\kappa)\}. \end{aligned} \tag{4.31}$$

For large SNR values that $\rho \rightarrow \infty$, (4.31) reduces to $\mathrm{P}\{y_2 > 0^+\} \rightarrow 1$. The reason behind this high outage probability is that $b < 0$ only holds for very large values of target data rates.

So far, it can be concluded that in CR-NOMA the parameters should be designed/chosen such that $\Delta\kappa < 0$ and $b > 0$ (case 4) in order to be able to significantly enhance the outage of the cognitive radio user.

Case 4: $\Delta\kappa < 0$ **and** $b > 0$**:**

In this case, it is highly probable that the channel gains of the primary and the cognitive radio user satisfy $x_1 < x_2$. Considering the condition on the SIC order for large values of SNR, Q_1 and Q_2 can be stated as follows

$$Q_1 = \mathrm{P}\{y_1 \leq \epsilon_1, y_2 > 1/(\rho\Delta\kappa)\}, \tag{4.32}$$

and

$$\begin{aligned} Q_2 =& \mathrm{P}\{y_1 > \epsilon_1, y_1 < a/b, y_2 > 1/(\rho\Delta\kappa)\} \\ \underset{\text{(b)}}{=}& \mathrm{P}\{\epsilon_1 < y_1 < a/b, y_2 > 1/(\rho\Delta\kappa)\}. \end{aligned} \tag{4.33}$$

Step (b) in (4.33) is due to the fact that $a/b > \epsilon_1$ always holds for $b > 0$. Furthermore, the condition on $y_2 > 1/(\rho\Delta\kappa) \to 0^+$ is always valid. Therefore, the outage probability of user 2 can be estimated in high-SNR regime by

$$P_2^{\text{out}} \approx F_{y_1}(a/b). \tag{4.34}$$

In addition, the SIC order condition reduces to $y_1 < y_2$ for this scenario with $\kappa_2 < \kappa_1$. Therefore, order statistics can be utilized to derive the CDFs, PDFs and the joint PDF of the ordered channel gains as follows

$$\begin{aligned}
F_{y_1}(Y) &= 1-(1-F_y(Y))^2 = 2F_y(Y)-F_y(Y)^2, && (4.35)\\
F_{y_2}(Y) &= F_y(Y)^2, && (4.36)\\
f_{y_1}(Y) &= f_y(Y), && (4.37)\\
f_{y_2}(Y) &= 2F_y(Y)f_y(Y), && (4.38)\\
f_{y_1,y_2}(Y_1,Y_2) &= 2f_y(Y_1)f_y(Y_2). && (4.39)
\end{aligned}$$

Here, we use (4.35) to reformulate (4.34) as follows

$$P_2^{\text{out}} \approx 2F_y(a/b) - F_y^2(a/b). \tag{4.40}$$

It can be seen from (4.40) that $P_2^{\text{out}} < F_y(a/b)(2-F_y(a/b))$, and since a/b includes $1/\rho \to 0^+$, this scenario is supposed to provide a much lower outage probability in comparison with case 3 for all the channel realizations of y_1. Consequently, it is required to design the system parameters such that $\Delta\kappa < 0$ and $b < 0$ to achieve the best possible NOMA gains.

(4.40) can be calculated using (4.18). However, this approximation does not provide an insightful expression to investigate the diversity gain. Therefore, in order to be able to analyze the diversity gain of this scheme, we assume that $h_k = g_k$ where $g_k \sim \mathcal{CN}(0,1)$. Hence, $f_y(Y) = e^{-Y}$ and $F_y(Y) = 1-e^{-Y}$. For the Rayleigh fading channel and the equivalent SIC order condition $y_1 < y_2$, Q_1 and Q_2 are given by

$$Q_1 = \mathrm{P}\{y_1 \le \epsilon_1, y_2 > y_1\}, \tag{4.41}$$

and

$$\begin{aligned}
Q_2 &= \mathrm{P}\{y_1 > \epsilon_1, y_1 < a/b, y_2 > y_1\}\\
&= \mathrm{P}\{\epsilon_1 < y_1 < a/b, y_2 > y_1\}. && (4.42)
\end{aligned}$$

By using (4.39) and the exponential PDF of the power of channel gains, the outage probability of the cognitive radio user at high-SNR regime can be stated as

$$\begin{aligned} P_2^{\text{out}} =& 2\Big(\int_0^{\epsilon_1} \int_{y_1}^{\infty} f_y(Y_1) f_y(Y_2) \mathrm{d}Y_1 \mathrm{d}Y_2 + \int_{\epsilon_1}^{a/b} \int_{y_1}^{\infty} f_y(Y_1) f_y(Y_2) \mathrm{d}Y_1 \mathrm{d}Y_2 \Big) \\ =& 1 - e^{-2a/b}. \end{aligned} \tag{4.43}$$

In addition, the exponential term of (4.43) can be approximated as $e^{-2a/b} \approx 1 - 2a/b$ since $a/b \to 0$ for $\rho \to \infty$. Therefore, the outage probability can be estimated as follows

$$P_2^{\text{out}} \approx 2a/b. \tag{4.44}$$

As previously mentioned, $a/b = \text{constant} \times \frac{1}{\rho}$. Therefore, diversity gain of the cognitive radio user is equal to one for a HWI aware scheme in which the system is designed based on the perfect knowledge of the HWI parameters. It can be seen that for the CR-NOMA, the performance of the stronger user is limited since it depends on the channel condition of the poor user. Note that diversity gain of the cognitive radio user without HWI is also equal to one [26] which emphasizes the robustness of NOMA against HWIs in high-SNR regime.

Chapter 5

Numerical Results

5.1 Ergodic Sum Rate Simulations for Fixed Power Allocation

The system model used for simulations in this part can be found in detail in Section 3.3 and the analysis is presented in Section 4.1. In addition, following assumptions are considered in this section. The path loss coefficient is equal to $\alpha = 3$, cell radius is considered to be $R = 1000$ m, and the distance between the kth user and the BS which is denoted by d_k is between 50 m and 1000 m. Moreover, a path loss of $\beta = 20$ dB at $d_0 = 50$ m is assumed. Therefore, path loss is obtained as $\frac{\beta}{(\frac{d}{d_0})^{\alpha}}$. Here, the ergodic sum rate for the two selected users is computed considering an opportunistic scenario ($\tilde{R}_k = R_k$).

5.1.1 Ideal Hardware

The ergodic sum rate of NOMA and OMA vs. SNR $= \rho = \frac{P}{\sigma_z^2}$ assuming ideal hardware is shown in Fig. 5.1. It can be seen that NOMA outperforms OMA in the high-SNR regime. For example, a gain of ≈ 1.5 bit/s/Hz in ergodic sum rate is achieved at $\rho = 40$ dB. Furthermore, NOMA does not show any improvement for small SNR values. Note that the SIC order is based on the channel gain normalized by noise.

5.1.2 Imperfect Hardware

The achievable ergodic sum rate given by (4.1) vs. SNR for both NOMA and OMA while considering HWI effects is shown in Fig. 5.2 for different values of $\kappa_{r,k}$. The SIC order is based on the gains as in $|h_k|^2/\Big(1+\rho|h_k|^2(\kappa_t+\kappa_{r,k})\Big)$, and thus, no outage occurs while detecting the signal of user 1 at user 2 as shown in (3.7). Based on results of Fig. 5.2, a

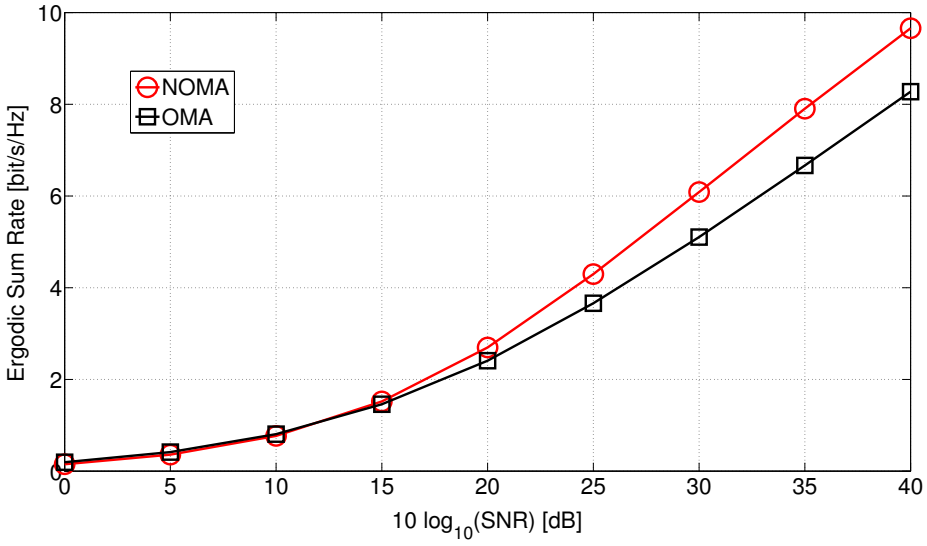

Fig. 5.1: Ergodic sum rate vs. SNR (ρ) without HWI.

degradation of ≈ 3.5 bit/s/Hz and more than 4 bit/s/Hz in sum rate can be observed at $\rho = 40$ dB for OMA and NOMA when HWI effects are taken into account.

In addition, the terms derived as ceilings for the ergodic sum rate in high-SNR regime as in (4.2) and (4.3) are depicted in Fig. 5.2. The ceiling values confirm that NOMA outperforms OMA for high values of SNR. For example, there is a gain of ≈ 0.4 bit/s/Hz for NOMA at $\rho = 40$ dB. Moreover, case 2 of NOMA in Fig. 5.2 shows a degradation of ≈ 0.3 dB at $\rho = 50$ dB compared to case 1. The larger value of $\kappa_{r,1}$ in spite of the lower $\kappa_{r,2}$ causes this degradation since the rate of the stronger user contributes more to the sum rate.

As discussed before, the new criterion on the decoding order prevents the occurrence of $R_{1\to 2} < R_1$ for the systems with imperfect hardware. However, for the decoding order based on $\frac{|h_k|^2}{\sigma_z^2}$, data rates of (3.5) are achievable in NOMA systems $\iff \kappa_{r,2} - \kappa_{r,1} \leq \frac{1}{\rho}(\frac{1}{|h_1|^2} - \frac{1}{|h_2|^2})$. Otherwise, NOMA system might be in outage. This outage probability vs. SNR for different values of κ_t and $\kappa_{r,k}$ is shown in Fig. 5.3. As can be seen, this outage reaches one for high values of SNR which can be explained by the previously introduced bound on the difference of $\kappa_{r,2}$ and $\kappa_{r,1}$. When $\rho \to \infty$, the aforementioned bound becomes tighter and in particular, $\frac{1}{\rho}(\frac{1}{|h_1|^2} - \frac{1}{|h_2|^2}) \to 0$. Therefore, it is less probable that $\kappa_{r,2} - \kappa_{r,1} \leq \frac{1}{\rho}(\frac{1}{|h_1|^2} - \frac{1}{|h_2|^2})$ holds. Clearly, these high values of outage probabilities in Fig. 5.3 are not negligible and it is important to modify the conventional SIC order for implementations in practice.

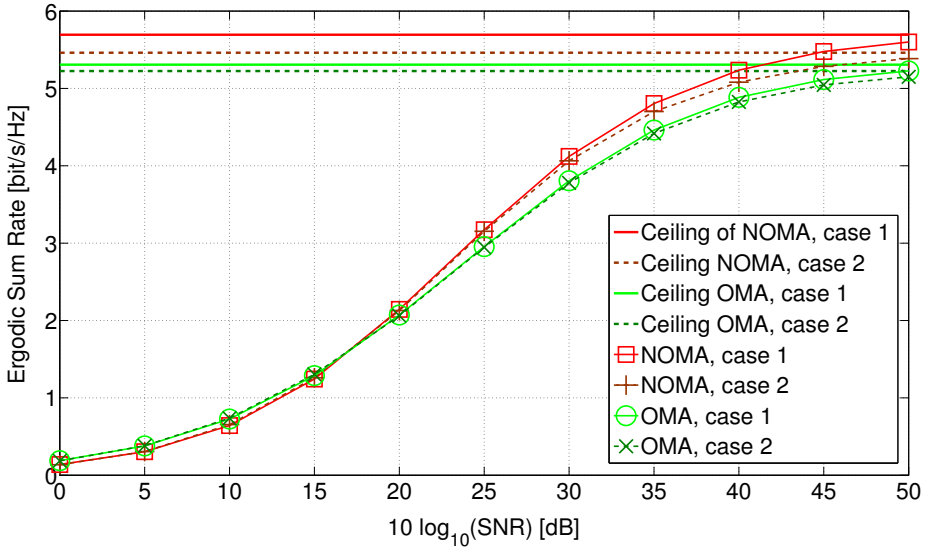

Fig. 5.2: Ergodic sum rate vs. SNR (ρ) for $\kappa_t = 0.01$ and different values of $\kappa_{r,k}$, case 1: $\kappa_{r,1} = 0.0085$ and $\kappa_{r,2} = 0.0264$, case 2: $\kappa_{r,1} = 0.0239$ and $\kappa_{r,2} = 0.0123$.

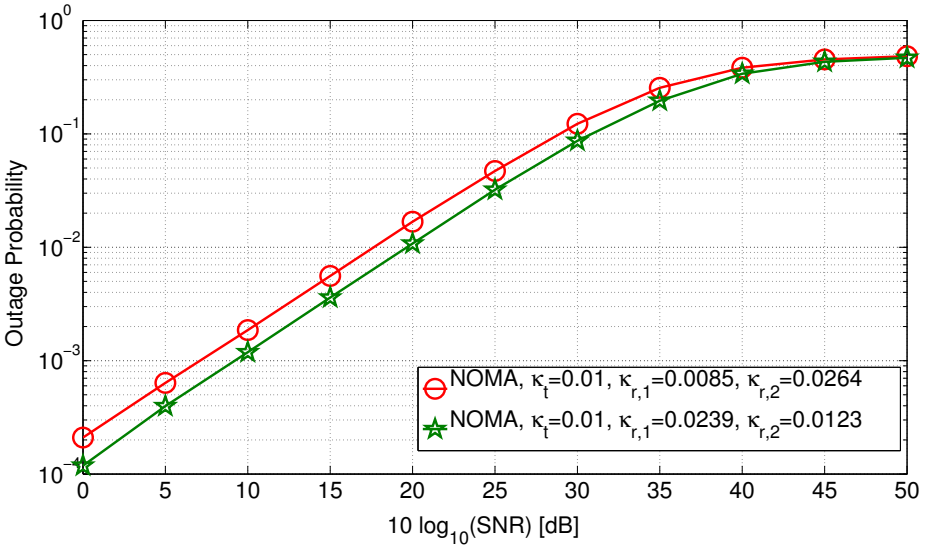

Fig. 5.3: Outage probability caused by inappropriate SIC order ($\frac{|h_k|^2}{\sigma_z^2}$) vs. SNR with imperfect hardware.

5.2 Outage Probability Simulations for Fixed Power Allocation

In this section, analytical results of Section 4.2 are verified by numerical simulations. Here, the same simulation parameters as in Section 5.1 are assumed.

In Fig. 5.4, the same target data rates are assumed for both NOMA users. Hence, as expected for an opportunistic scenario, the outage probability of the stronger user is lower than that of the user with poor channel condition for all SNRs. Furthermore, a

good match between the analytical results and the simulation results can be observed. Moreover, it can be seen that the analytical solution provided by power series which is referred to as method 1 is more accurate. Note that these analytical estimations are derived only for large values of SNR. That is why they do not match the simulation results for low values of SNR.

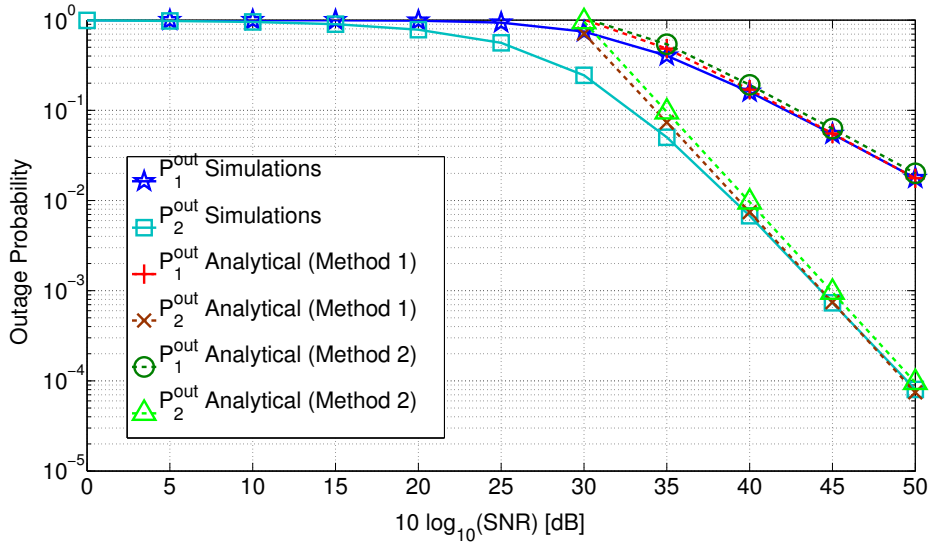

Fig. 5.4: Outage probability vs. SNR for $\kappa_t = 0.01$, $\kappa_{r,(1)} = 0.0085$, $\kappa_{r,(2)} = 0.0264$ and $\tilde{R}_1 = \tilde{R}_2 = 2$.

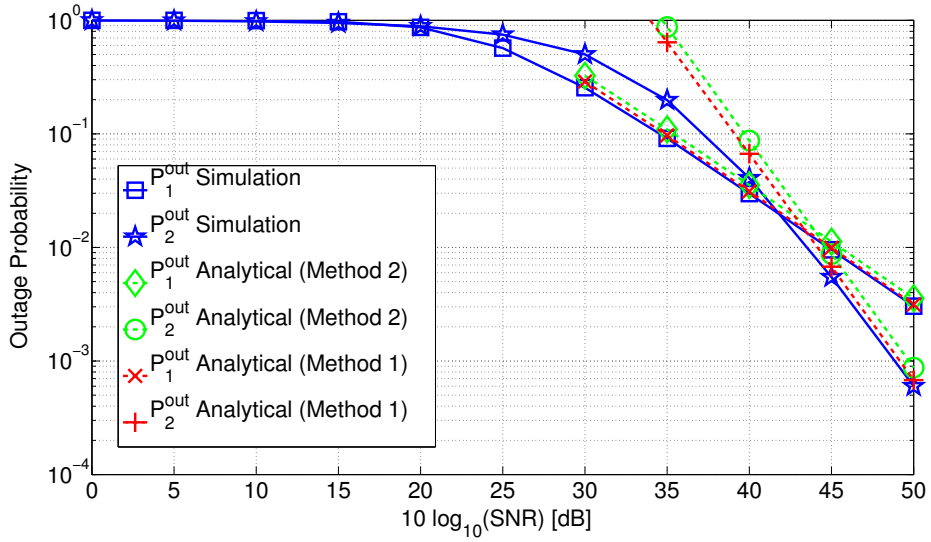

Fig. 5.5: Outage probability vs. SNR for $\kappa_t = 0.01$, $\kappa_{r,(1)} = 0.0085$, $\kappa_{r,(2)} = 0.0264$ and $\tilde{R}_1 = 1.5$ and $\tilde{R}_2 = 2.5$.

In Fig. 5.5, outage probability vs. SNR is depicted while different target data rates are selected for NOMA users. Here, when $\tilde{R}_1 = 2$ of Fig. 5.4 changes to $\tilde{R}_1 = 1.5$, the outage probability of user 1 significantly decreases, e.g., it becomes 2×10^{-3} from 2×10^{-2} at

the SNR of 50 dB. It can also be seen that for a specific range of SNRs between 20 dB and 40 dB, user 1 has even a lower outage than user 2. The reason is that $\tilde{R}_1 = 1.5$ is a reasonable choice for the weak user in the case under study. However, $\tilde{R}_2 = 2.5$ is close to the rate which can be achieved by user 2 for large SNR values. These results indicate that the right choice of target data rates can highly improve the system performance of NOMA.

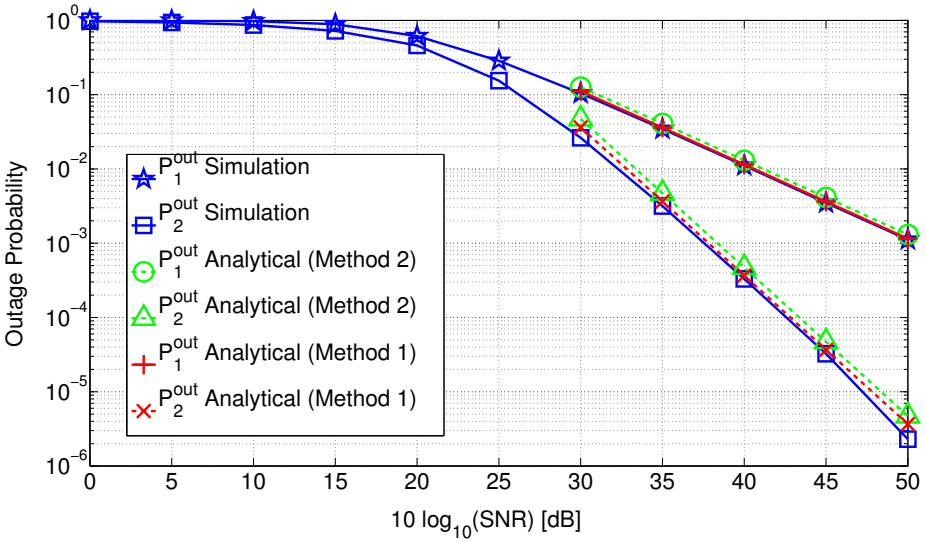

Fig. 5.6: Outage probability vs. SNR for $\kappa_t = 0.01$, $\kappa_{r,(1)} = 0.0239$, $\kappa_{r,(2)} = 0.0123$, $\tilde{R}_1 = \tilde{R}_2 = 1$.

In addition, outage probability vs. SNR with $\tilde{R}_1 = \tilde{R}_2 = 1$ is depicted in Fig. 5.6. By comparing the results of Fig. 5.6 with Fig. 5.4 and 5.5, it can be seen that the amount of outage highly depends on the target data rates. In Fig 5.6, where $\tilde{R}_1$ and $\tilde{R}_2$ have the smallest value among all simulations, outage probabilities approach 2×10^{-6} and 10^{-3} in spite of the worse HWI parameters. Remind the fact that HWI parameter of the stronger user has more influence on the system performance.

Clearly, Figs. 5.4, 5.5 and 5.6 support the accuracy of the approximations provided in Section 4.2. Moreover, method 1 presents a better estimation for the outage performance of NOMA in high-SNR regime. Note that these approximations are only valid for high-SNR because only in that case, the exponential function can be estimated by two terms (see Section 4.2). In addition, increasing the terms in this approximation results only in a slight improvement. That is why two terms ($N = 1$) were considered for all simulations in this section.

In Fig. 5.7, outage probabilities of NOMA and OMA are compared for perfect and imperfect hardware. Clearly, including HWIs results in performance degradation of both NOMA and OMA. However, this degradation caused by imperfect hardware is not significant, e.g., the outage probabilities are increased by $\approx 4 \times 10^{-3}$, 10^{-2} and

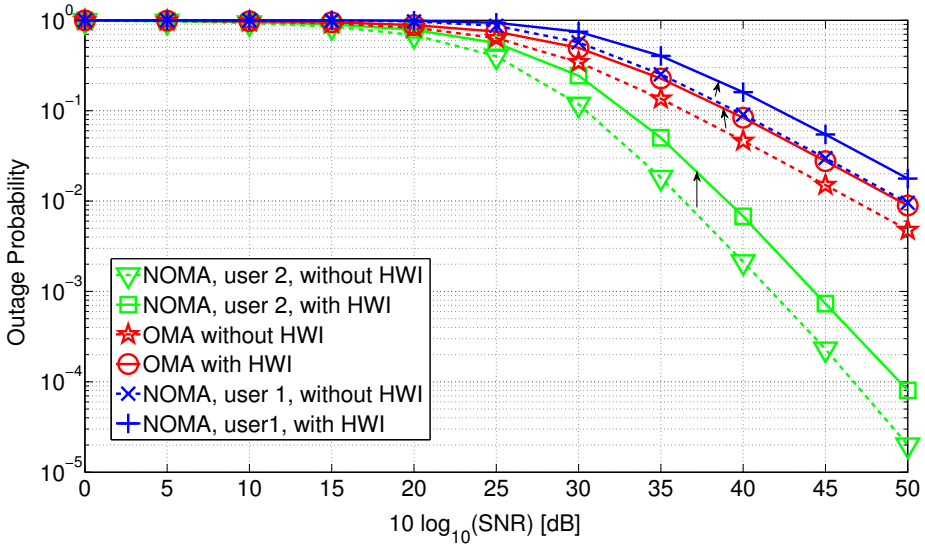

Fig. 5.7: Outage probability vs. SNR for $\kappa_t = 0.01$, $\kappa_{r,(1)} = 0.0085$, $\kappa_{r,(2)} = 0.0264$, $\tilde{R}_1 = \tilde{R}_2 = 2$.

6×10^{-5} at $\rho = 50$ dB for the OMA user, the weak and the strong users of NOMA, respectively. Moreover, as can be observed from Fig. 5.7 and as it was analytically shown in Section 4.2, the diversity gains remain unchanged in the presence of HWIs which implies the robustness of NOMA against HWIs.

In order to further investigate the impact of HWIs on outage probability, in Fig. 5.8, P^{out} for NOMA and OMA vs. $\kappa_{r,(1)}$ is shown at SNR=50 dB. Note that for small values of SNR, outage probability is almost one, and that is why $\rho = 50$ dB is considered here. Fig. 5.8 indicates the fact that the performance of the stronger user is more robust to the changes in HWI parameters. However, the performance of OMA user and the weaker NOMA user are showing almost similar degradation. For example, the difference between the maximum and minimum outage probabilities for OMA user and the weak NOMA user are ≈ 0.005 and 0.003, respectively. Therefore, it can be concluded that NOMA is a more robust multiple access technology than OMA for implementations with imperfect hardware.

In addition, Fig. 5.9 shows the outage probability vs. κ_t. The results of this figure confirm that the outage probability of the stronger user of NOMA is significantly more robust with respect to the HWI effects than the weaker NOMA user and OMA user for different values of HWI parameters $\kappa_{r,(k)}$ and κ_t. In addition, increasing the BS HWI parameter is more destructive for the weak NOMA user compared to the OMA user.

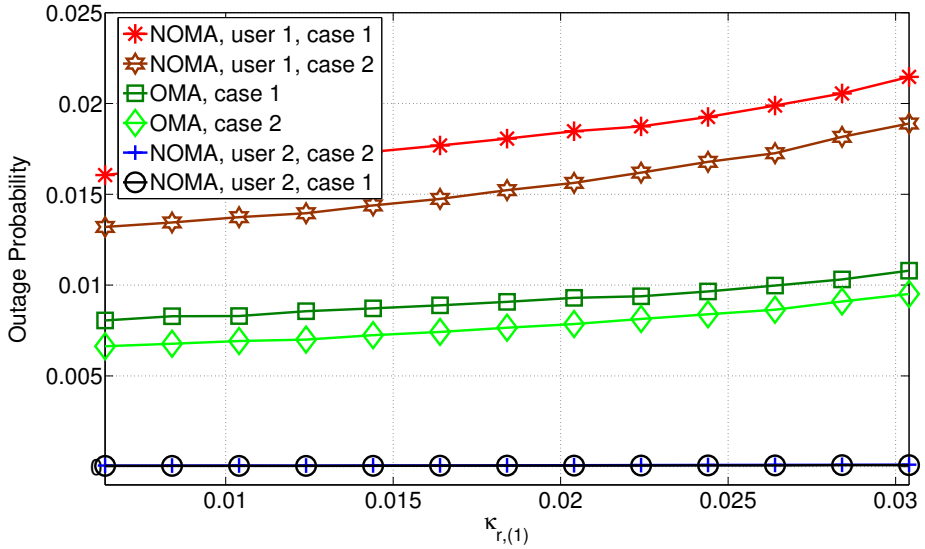

Fig. 5.8: Outage probability vs. $\kappa_{r,(1)}$ for SNR=50 dB, $\tilde{R}_1 = \tilde{R}_2 = 2$, case 1: $\kappa_t = 0.0085$ and $\kappa_{r,(2)} = 0.0264$, case 2: $\kappa_t = 0.01$ and $\kappa_{r,(2)} = 0.01$.

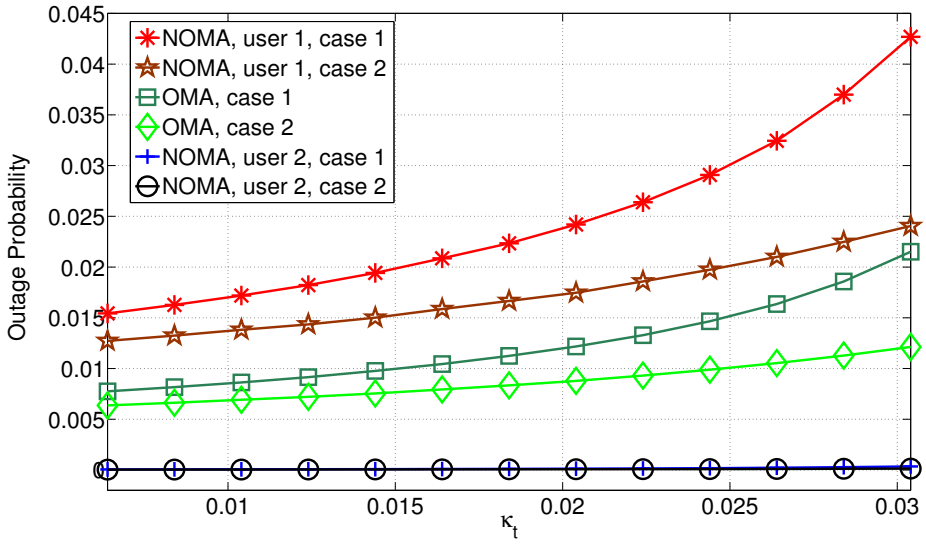

Fig. 5.9: Outage probability vs. κ_t for SNR=50 dB, $\tilde{R}_1 = \tilde{R}_2 = 2$, case 1: $\kappa_{r,(1)} = 0.0085$ and $\kappa_{r,(2)} = 0.0264$, case 2: $\kappa_{r,(1)} = 0.01$ and $\kappa_{r,(2)} = 0.01$.

5.3 Outage Probability Simulations for Cognitive Radio NOMA

In this section, the outage performance of CR-NOMA is investigated. Here, we assume the same simulation parameters as in Section 5.1. Fig. 5.10 shows the outage probability of the cognitive radio user vs. SNR where both Rayleigh fading and path loss are taken into account in channel gains. As can be seen, the outage probability is always equal

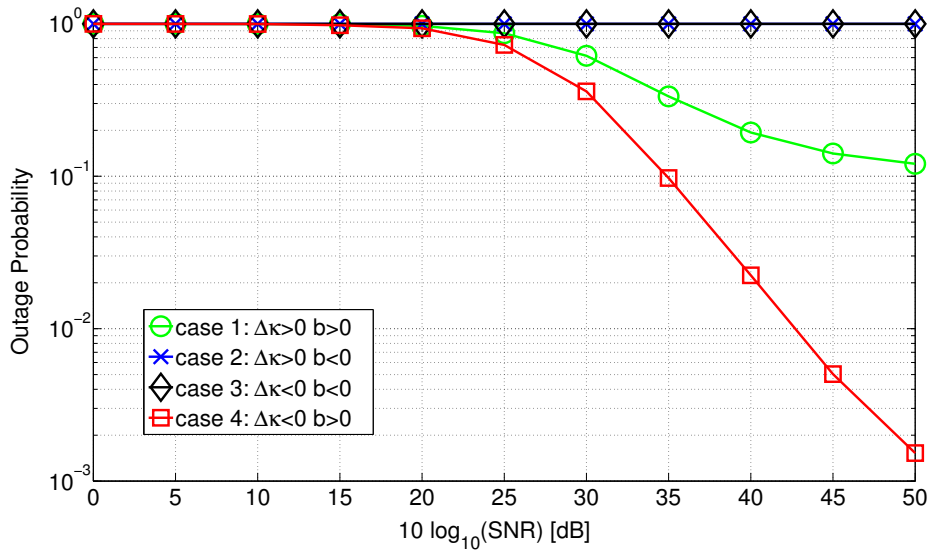

Fig. 5.10: Outage probability of cognitive radio user vs. SNR for channels with path loss and Rayleigh fading gains, $\kappa_t = 0.01$, $\tilde{R}_1 = \tilde{R}_2 = 2$ for $b > 0$, $\tilde{R}_1 = \tilde{R}_2 = 3$ for $b < 0$, $\kappa_{r,1} = 0.0085$ and $\kappa_{r,2} = 0.0264$ for $\Delta\kappa > 0$, $\kappa_{r,1} = 0.0264$ and $\kappa_{r,2} = 0.0085$ for $\Delta\kappa < 0$.

to one, for $b < 0$. The reason is the large target data rates which result in negative values of b as discussed in Section 4.3. Furthermore, when the system parameters are selected such that $\Delta\kappa > 0$, satisfying $x_1 < x_2$ requires very poor channels for the primary user and very strong channels for the cognitive radio user. Additionally, performance of the cognitive radio user depends on the channel condition and HWI parameter of the primary user. Therefore, in spite of $b > 0$ in case 3, the outage probability values are still large even in high-SNR region, e.g., ≈ 0.1 at $\rho = 50$ dB. To this end, case 4 which satisfies both $b > 0$ and $\Delta\kappa < 0$ is supposed to provide the best outage performance which is confirmed by the results of Fig. 5.10. Clearly, the simulation results provided by Fig. 5.10 support the accuracy of the analysis performed in Section 4.3 for channels consisting both Rayleigh fading gains and path loss.

In Fig. 5.11, the outage probability of the cognitive radio user vs. SNR is depicted for case 4 considering Rayleigh fading channel gains. As can be observed, the analytical results of (4.43) and (4.44) perfectly match the simulation results in high-SNR regime. Clearly, the diversity gain of the cognitive radio user is equal to one. Therefore, CR-NOMA shows robustness in a HWI aware system.

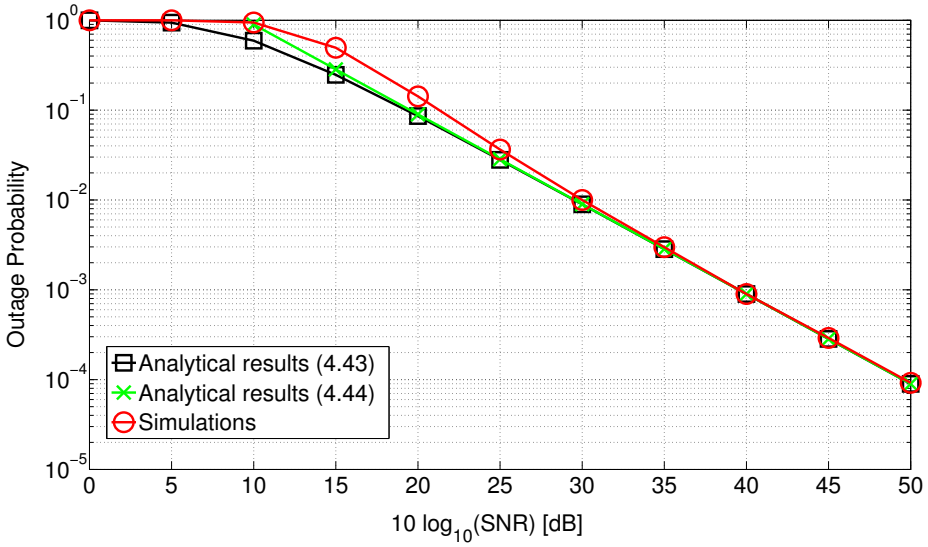

Fig. 5.11: Outage probability of cognitive radio user vs. SNR for Rayleigh fading channel, $\kappa_t = 0.01$, $\kappa_{r,1} = 0.0264$, $\kappa_{r,2} = 0.0085$ and $\tilde{R}_1 = \tilde{R}_2 = 2$.

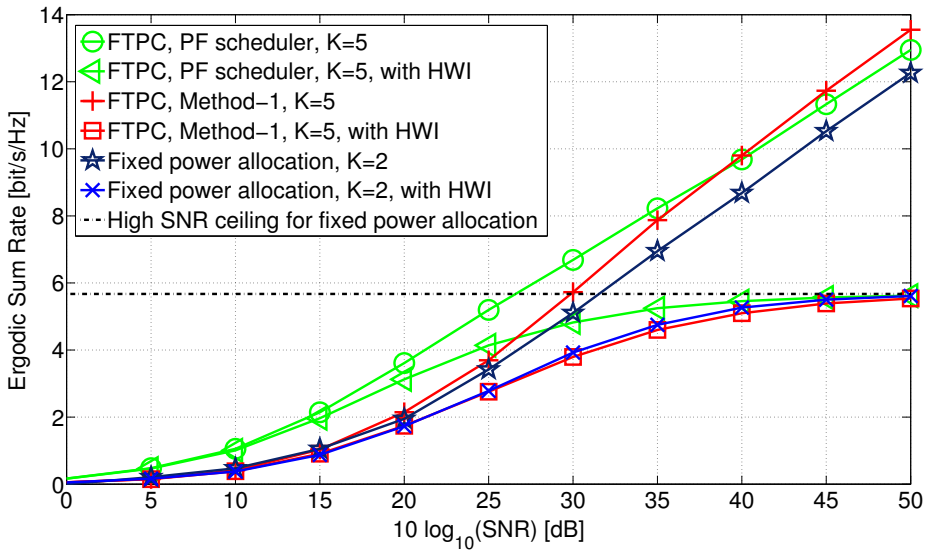

Fig. 5.12: Ergodic sum rate vs. SNR for $\kappa_t = \kappa_{r,1} = \kappa_{r,2} = 0.01$.

5.4 Ergodic Sum Rate Simulations for Fractional Transmission Power Allocation

In this section, ergodic sum rates are evaluated for the following scenarios: PF scheduling with FTPC as power allocation, pairing based on the most distinctive channel gains (referred to as method-1 in Fig. 5.12) and FTPC, and finally, the one studied in the last sections with fixed power allocation and random scheduling. For more details see Section 2. In these simulations, $R = 5$ m, $\alpha = 3$, $\kappa_t = \kappa_{r,1} = \kappa_{r,2} = 0.01$, $T = 10$ and

$\alpha_{FTPC} = 0.4$. In addition, we assume that there are $K = 5$ uniformly distributed users in cell among which 2 users are selected by scheduler to perform NOMA.

The results in terms of ergodic sum rate vs. SNR with and without HWIs are shown in Fig. 5.12. As expected, PF scheduling with FTPC outperforms other scenarios since it adopts more powerful scheduling and power allocation methods. In addition, the simple scenario with random scheduling and fixed power allocation achieves the smallest sum rate. It is worth mentioning that pairing based on the most distinctive channel gains is optimum in terms of sum rate only if a fixed power allocation is adopted. Therefore, when FTPC is used, this pairing scheme is no longer the optimum scheduler. Fig. 5.12 also shows the high-SNR ceiling which was derived for NOMA with random scheduling and fixed power allocation. It can be seen that the performance of all scenarios with HWI in high-SNR regime is limited. Thus, this ceiling can be used to roughly describe the performance of NOMA in terms of system throughput in high-SNR regime regardless of the scheduling and power allocation methods.

Chapter 6

Conclusion

In this thesis, we investigated the effects of transceiver HWIs on NOMA by analysis and simulation. A ceiling was derived for the ergodic sum rate of an opportunistic NOMA scenario adopting random scheduling and fixed power allocation. This ceiling shows that the high gains of NOMA saturate at high-SNR regime where HWIs are present. However, NOMA still outperforms OMA at the moderate-to-high SNR region in terms of spectral efficiency. It was also shown by simulations that it is vital to modify the conventional SIC order for avoiding the occurrence of outages.

Furthermore, a closed-form expression was derived for the outage probability of a QoS-based NOMA system using the same scheduling and power allocation. The asymptotic study of this outage probability indicates that the diversity gain of the weaker user and the stronger user are one and two, respectively. These values confirm the robustness of NOMA with respect to HWIs since the diversity gains of NOMA with HWIs remain the same as the diversity gains of NOMA with ideal hardware. It is worth mentioning that the outage performance of each user in QoS-based NOMA depends on the decoding order of that user. Moreover, outage probability of both NOMA users are highly influenced by the values of target data rates. In other words, the appropriate choice of predefined data rates results in NOMA performance improvements. It was also shown that the stronger user of NOMA is more robust than OMA user with respect to changes in HWI parameters. This robustness is an important feature in system-level design, particularly because the stronger user has a significant impact on the total system throughput of the cell.

Moreover, we defined two parameters based on the HWI coefficients and target data rates in order to categorize CR-NOMA into four cases and analyze the outage probability performance in high-SNR regime. It was shown that the best outage probabilities are achieved for the case where both of these introduced parameters have negative values, i.e., $\Delta\kappa < 0$ and $b < 0$. Therefore, the outage performance of this case was studied in detail and a closed-form expression for the outage probability of the cognitive radio user was derived, where Rayleigh fading channels were assumed. Based on the derived

outage probability, we demonstrated that the diversity gain of the cognitive radio user is equal to one. Clearly, the performance of the cognitive radio user is highly influenced by the HWI parameter and channel condition of the primary user. Furthermore, since the diversity gain of the cognitive radio user in a system with ideal hardware is also equal to one [26], the robustness of CR-NOMA in the presence of HWIs can be concluded.

From the results provided in this thesis, the importance of considering the effect of HWI on designing and investigating the NOMA systems becomes clear. Therefore, studying the performance of other NOMA schemes, e.g., multi-carrier and MIMO-NOMA can be considered as the future works. More importantly, designing power allocation and scheduling methods while taking the HWI effects into account are interesting topics to be investigated in future.

Appendices

A. Rate Region of Multiple Access Channels

Multiple Access Channel (MAC) is used to model the uplink multiuser systems. For a MAC with two users, the achievable rate region is determined by the following equations.

$$R_1 < \log_2(1 + \frac{P_1}{\sigma_z^2}), \tag{A.1}$$

$$R_2 < \log_2(1 + \frac{P_2}{\sigma_z^2}), \tag{A.2}$$

$$R_1 + R_2 < \log_2(1 + \frac{P_1 + P_2}{\sigma_z^2}). \tag{A.3}$$

This rate region is shown in Fig. A.1. Note that the rate region can similarly be extended for a higher number of users. Achieving the border of this region can be done by SIC. Particularly, the points between B and C can be achieved if for θ% of a time slot, we first detect user 1 and for remaining time we detect the 2nd user first (time sharing and non-orthogonal). Therefore, the decoding order does not affect the sum rate of an uplink scenario.

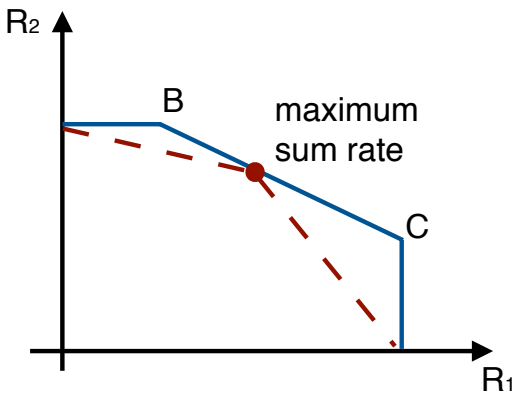

Fig. A.1: Rate region of MAC. The brown dashed line and the solid blue line represent OMA and NOMA rate regions, respectively.

Clearly, non-orthogonal multiplexing provides a wider range of users' data rates which maximize the sum rate (all the points on B-C). This wider rate region for NOMA implies a

better trade-off between achieving a high sum rate and user fairness. However, for TDMA and FDMA, there exist only one point on B-C for which OMA can reach the maximum sum rate.

B. Randomly Deployed Users

The PDF of the channel gains in Section 3.1 which is introduced in [27], is derived for a case where the users are uniformly distributed on disc D. This means that the $(x, y) \in D$[1] is uniformly distributed, and not the distance between the BS and user d. Therefore, for a disc with radius R and $f_{x,y}(X, Y)$ as the joint uniform distribution of $x,\ y$:

$$f_{x,y}(X, Y) = \text{constant} = k. \tag{B.4}$$

We know that $\int\int f_{x,y}(X, Y)\mathrm{d}x\mathrm{d}y = 1$, so we can write

$$\int\int k\mathrm{d}x\mathrm{d}y = k\pi R^2 = 1 \Rightarrow k = f_{x,y}(X, Y) = \frac{1}{\pi R^2}. \tag{B.5}$$

From cartesian (x, y), to polar coordinate (z, θ)

$$z = \sqrt{x^2 + y^2},\quad \theta = \arctan(\frac{y}{x}), \tag{B.6}$$

$$\mathrm{d}x\mathrm{d}y = z\mathrm{d}z\mathrm{d}\theta. \tag{B.7}$$

In addition, assuming that $P(\cdot)$ represents the probability, we have

$$P(X \le x \le X + \mathrm{d}x, Y \le y \le Y + \mathrm{d}y) = P(Z \le z \le Z + \mathrm{d}z, \Theta \le \theta \le \Theta + \mathrm{d}\theta). \tag{B.8}$$

We know that

$$P(X \le x \le X + \mathrm{d}x, Y \le y \le Y + \mathrm{d}y) = f_{x,y}(X, Y)\mathrm{d}x\mathrm{d}y. \tag{B.9}$$

In addition, using (B.5), (B.7), (B.8) and (B.9), we have

$$\frac{1}{\pi R^2}\mathrm{d}x\mathrm{d}y = \frac{1}{\pi R^2}z\mathrm{d}z\mathrm{d}\theta. \tag{B.10}$$

Therefore,

$$f_{z,\theta}(Z, \Theta) = \frac{z}{\pi R^2}. \tag{B.11}$$

[1] x and y present the axes of the cartesian coordinates.

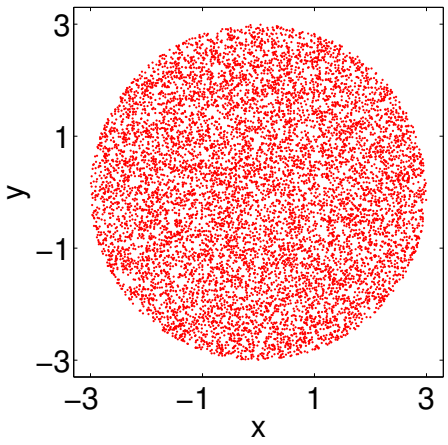

Fig. B.2: Uniform distribution of user locations in a disc with $R = 3$.

To calculate the marginal distributions, we can write:

$$f_z(Z) = \int_{\theta=0}^{2\pi} \frac{z}{\pi R^2} \mathrm{d}\theta = \frac{2z}{R^2}, \tag{B.12}$$

$$f_\theta(\Theta) = \int_{z=0}^{R} \frac{z}{\pi R^2} \mathrm{d}z = \frac{1}{2\pi}. \tag{B.13}$$

Implementing the uniform distribution of $f_\theta(\Theta)$ is straightforward in MATLAB. In order to implement the distribution of $f_z(Z)$, we use the inversion method. The inversion method relies on the principle that continuous cumulative distribution functions (CDFs) range uniformly over the open interval $(0, 1)$. If u is a uniform random number on $(0, 1)$, then $z = F^{-1}(u)$ generates a random number z from any continuous distribution with the specified CDF F From (B.12),

$$F_z(r) = P(z \leq r) = \int_{z=0}^{r} f_z(Z)\mathrm{d}z = \frac{2}{R^2}\frac{r^2}{2} = \frac{r^2}{R^2}. \tag{B.14}$$

Hence, $r = R\sqrt{F_z(r)}$. The inverse cumulative pdf, $F_z(r)$ can be simply implemented using rand function in MATLAB. Moreover, $x = r\cos\theta$, $y = r\sin\theta$. Fig. B.2 shows the distribution of the points generated by this code. Clearly, d, i.e., the distance between the BS and user can be simply calculated from the locations of the users or equally by a set of (x, y).

Bibliography

[1] S. Cherry, “Edholm’s Law of Bandwidth,” *IEEE Spectrum*, vol. 41, no. 7, pp. 58–60, 2004.

[2] Z. Wei, J. Yuan, D. W. K. Ng, M. Elkashlan, and Z. Ding, “A Survey of Downlink Non-orthogonal Multiple Access for 5G Wireless Communication Networks,” *accepted by ZTE Communications. [Online]. Available: https://arxiv.org/abs/1609.01856*, 2016.

[3] Z. Ding, X. Lei, G. K. Karagiannidis, R. Schober, J. Yuan, and V. Bhargava, “A Survey on Non-Orthogonal Multiple Access for 5G Networks : Research Challenges and Future Trends,” *to appear in IEEE Journal on Selected Areas in Communications. [Online]. Available: https://arxiv.org/abs/1706.05347*, 2017.

[4] P. Xu, Z. Ding, X. Dai, and H. V. Poor, “A New Evaluation Criterion for Non-orthogonal Multiple Access in 5G Software Defined Networks,” *IEEE Access*, vol. 3, pp. 1633–1639, 2015.

[5] A. Benjebbour, Y. Saito, Y. Kishiyama, A. Li, A. Harada, and T. Nakamura, “Non-Orthogonal Multiple Access (NOMA) for Cellular Future Radio Access,” *IEEE 77th Vehicular Technology Conference (VTC Spring), Dresden*, 2013, pp. 1–5.

[6] Y. Saito, A. Benjebbour, Y. Kishiyama, T. Nakamura, “System-level performance evaluation of downlink non-orthogonal multiple access (NOMA),” in *IEEE 24th Annual International Symposium on Personal, Indoor, and Mobile Radio Communications (PIMRC)*, London, 2013, pp. 611–615.

[7] A. Benjebbour, A. Li, Y. Kishiyama, H. Jiang, and T. Nakamura, “System-Level Performance of Downlink NOMA Combined with SU-MIMO for Future LTE Enhancements,” *IEEE Globecom Workshops (GC Wkshps), Austin, TX*, 2014, pp. 706–710.

[8] M. Al-Imari, P. Xiao, M. A. Imran, and R. Tafazolli, “Uplink Non-Orthogonal Multiple Access for 5G Wireless Networks,” *11th International Symposium on Wireless Communications Systems (ISWCS), Barcelona*, 2014, pp. 781–785.

[9] Z. Ding, M. Peng, and H. V. Poor, "Cooperative Non-Orthogonal Multiple Access in 5G Systems," *IEEE Communications Letters*, vol. 19, no. 8, pp. 1462–1465, 2015.

[10] Y. Lan, A. Benjebboiu, X. Chen, A. Li and H. Jiang, "Considerations on Downlink Non-orthogonal Multiple Access (NOMA) Combined with Closed-Loop SU-MIMO," *8th International Conference on Signal Processing and Communication Systems (ICSPCS), Gold Coast, QLD*, 2014, pp. 189–196.

[11] Z. Chen, Z. Ding, S. Member, and X. Dai, "A Mathematical Proof of the Superiority of NOMA Compared to Conventional OMA," *submitted to IEEE Transactions on Signal Processing. [Online]. Available: https://arxiv.org/abs/1612.01069v1*, 2016.

[12] N. Otao, Y. Kishiyama, and K. Higuchi, "Performance of Non-orthogonal Multiple Access with SIC in Cellular Downlink Using Proportional Fair-Based Resource Allocation," *International Symposium on Wireless Communication Systems (ISWCS), Paris*, 2012, pp. 476–480.

[13] Y. Sun, D. Wing, K. Ng, Z. Ding, and R. Schober, "Optimal Joint Power and Subcarrier Allocation for Multicarrier Non-Orthogonal Multiple Access Systems," *IEEE Global Communications Conference (GLOBECOM), Washington, DC*, 2016, pp. 1–6.

[14] Z. Ding, Z. Yang, P. Fan, and H. V. Poor, "On the Performance of Non-orthogonal Multiple Access in 5G Systems with Randomly Deployed Users," *IEEE Signal Processing Letters*, vol. 21, no. 12, pp. 1501–1505, 2014.

[15] Z. Yang, Z. Ding, P. Fan, and G. K. Karagiannidis, "On the Performance of 5G Non-Orthogonal Multiple Access Systems with Partial Channel Information," *IEEE Transactions on Communications*, vol. 64, no. 2, pp. 654–667, 2015.

[16] E. Björnson, J. Hoydis, and M. Kountouris, "Massive MIMO Systems with Non-Ideal Hardware: Energy Efficieny, Estimation and Capacity Limits," *IEEE Transactions on Information Theory*, vol. 60, no. 11, pp. 7112–7139, 2014.

[17] J. Zhang, L. Dai, X. Zhang, and E. Bj, "Achievable Rate of Rician Large-Scale MIMO Channels with Transceiver Hardware Impairments," *IEEE Transastions on Vehicular Technology*, vol. 65, no. 10, pp. 8800–8806, 2016.

[18] K. Higuchi and A. Benjebbour, "Non-orthogonal Multiple Access (NOMA) with Successive Interference Cancellation for Future Radio Access," *IEEE Transactions on Communications*, no. 3, pp. 403–414, 2015.

[19] Z. Ding, P. Fan, and H. V. Poor, "User Pairing in Non-Orthogonal Multiple Access Downlink Transmissions," *IEEE Global Communications Conference (GLOBECOM), San Diego, CA*, 2015, pp. 1–5.

[20] H. Kim and Y. Han, "A Proportional Fair Scheduling for Multicarrier Transmission Systems," *IEEE Communications Letters*, vol. 9, no. 3, pp. 210–212, 2005.

[21] S. Tim, *RF Imperfections in High-rate Wireless Systems*, 1st ed. Dordrecht, The Netherlands: Springer, 2008.

[22] C. Studer, M. Wenk and A. Burg, "MIMO Transmission with Residual Transmit-RF Impairments," *International ITG Workshop on Smart Antennas (WSA), Bremen*, 2010, pp. 189–196.

[23] P. Zetterberg, "Experimental Investigation of TDD Reciprocity-based Zero-forcing Transmit Precoding," *EURASIP Journal on Advances in Signal Processing*, 2011.

[24] M. Wenk, "MIMO-OFDM Testbed: Challenges, Implementations, and Measurement Results," *(Microelectronics). Konstanz, Germany: Hartung-Gorre*, 2010.

[25] W. Zhang, "A General Framework for Transmission with Transceiver Distortion and Some Applications," *IEEE Transactions on Communications*, vol. 60, no. 2, pp. 384–399, 2012.

[26] Z. Ding, P. Fan, and H. V. Poor, "Impact of User Pairing on 5G Non-orthogonal Multiple Access Downlink Transmissions," *IEEE Transactions on Vehicular Technology*, vol. 65, no. 8, pp. 6010–6023, 2016.

[27] Z. Ding and H. V. Poor, "Cooperative Energy Harvesting Networks with Spatially Random Users," *IEEE Signal Processing Letters*, vol. 20, no. 12, pp. 1211–1214, 2013.